International Journal of Theoretical Physics (2026) 65:59
https://doi.org/10.1007/s10773-025-06183-3

RESEARCH

Abundant Soliton Solutions to the New Modified Spectral KdV Equation in Ocean Engineering with Bifurcation Analysis

Md Nur Hossain[1,2] · I. Abouelfarag[3] · Abdulkafi Mohammed Saeed[4] · K. El-Rashidy[5] · M. Mamun Miah[6,7] · Wen-Xiu Ma[8,9,10]

Received: 18 March 2025 / Accepted: 20 October 2025

Abstract

The transformation of water waves in shallow regions is a complex phenomenon. As waves reach the beach, they undergo many processes, including shoaling, refraction, diffraction, and breaking. The importance of precisely forecasting wave patterns in shallow water areas is underscored by their influence on sediment transport, circulation, and other nearshore processes. This work looks at the one-dimensional modified spectral Korteweg–de Vries (mSKdV) equation as a mathematical framework to improve the comprehension of nonlinear wave transformation in shallow water. The research provides insights into the influence of changing bathymetry and nonlinearity on wave evolution along the beach. The unified method and the $\left(\frac{G'}{G}, \frac{1}{G}\right)$ method are two effective techniques that are utilized in order to derive soliton solutions for this equation. A bifurcation analysis is conducted to ascertain the phase portrait of this equation. Beyond the direct observations, a linear stability analysis was also performed. This crucial step further confirms and quantifies how the stability of our solutions changes across various bathymetries. This analysis provides a rigorous mathematical framework, reflecting the solutions' resilience and behavior under different underwater topographies. A synthesis of three-dimensional plots, modified two-dimensional plots concerning the time variable t, and density plots is employed to illustrate the precise solutions obtained. These diagrams illustrate the transition from the shallow water zone to the shoreline. Various soliton phenomena have been observed, including periodic solitons, bright and dark solitons, periodic breathers, quasi-breathers, breathers, and kinks. This discovery significantly advances the development of soliton solutions for the mSKdV equation. It also offers significant insights on the spectrum wave height and setup that unfold in coastal engineering, especially in regions with shallow seas.

Keywords Shallow water waves · The $\left(\frac{G'}{G}, \frac{1}{G}\right)$ method · The unified method · Modified spectral Korteweg-de Vries equation · Bifurcation · Soliton solutions

Extended author information available on the last page of the article

Published online: 16 February 2026

1 Introduction

Essential tools for precisely simulating a wide spectrum of complicated and real-world events across scientific and technical fields are nonlinear partial differential equations (PDEs). Offering deeper and more realistic insights into these fields, nonlinear PDEs skillfully reflect the underlying complexity of systems including turbulent fluid flows, chaotic atmospheric behavior, nonlinear optical waves, and biological pattern development unlike their linear counterparts [1–9]. Crucially in fields including plasma physics, shallow water dynamics, fiber optics, and nonlinear acoustics, these equations are fundamental in analyzing nonlinear behaviors including shock waves, soliton interactions, breather dynamics, modulation instability, and phase bifurcations [1, 2, 4–6, 8, 11]. Studies on extended Korteweg–de Vries and coupled Whitham–broer–Kaup-type equations have shown, for example, diverse wave structures comprising multi-soliton complexes, chaotic waveforms, and stochastic responses [5–7, 14]. Under external influences, nonlinear PDEs assist to clarify events including phase transitions, instability mechanisms, and pattern development in materials science and wave mechanics [10, 12, 13]. These difficulties also encourage the growth of sophisticated analytical techniques including fractional calculus, bifurcation theory, and symbolic computation as well as computational methods, so increasing our capacity to forecast, control, and maximize nonlinear behavior in useful contexts including structural analysis, advanced optics, and climate modeling [10–15]. As such, nonlinear PDEs remain a fundamental element of contemporary mathematical physics, bridging the distance between theoretical discoveries and engineering application.

Among different fields the coastal engineering is a critical field that focuses on designing coastal structures and mitigating threats to coastal regions. One key area of study in this field is the behavior of shallow water waves, as these areas are highly dynamic due to factors like bottom slope and wave-breaking phenomena. In shallow water, waves break and entrain air bubbles and sediment into the water column, leading to complex interactions that reduce wave height and set-up over time until the waves eventually dissipate [16–23]. To accurately measure and predict the behavior of shallow water waves, it is essential to study equations that characterize their dynamics, such as the mSKdV equation. This equation is particularly effective in describing soliton dynamics, which play a significant role in shallow water environments. Understanding these dynamics provides valuable insights for designing resilient coastal infrastructure and managing coastal processes effectively. Also, the mSKdV equation is an important equation in the analysis of wave propagation in shallow water, particularly when examining the behavior of nonlinear waves. By assuming one-dimensional wave propagation and slowly varying water depth, the Boussinesq equations can be reduced to this spectral form. In a normalized setting, the mSKdV equation can be expressed using representative quantities. The mSKdV equation captures the dynamics of wave evolution, focusing on the balance between nonlinear effects and wave dispersion. It is typically formulated as follows [24]**:**

$$\xi_t + \sqrt{h}\xi_x + \frac{h_x}{4\sqrt{h}}\xi + \frac{3\varepsilon}{2\sqrt{h}}\xi\xi_x + \frac{\gamma^2 h^{\frac{5}{2}}}{6}\xi_{xxx} = 0 \tag{1}$$

where h is the water depth, ε is the wave amplitude, $\gamma = k_0 h_0$; k_0 incident wave number, h_0 incident water depth, h_x is the beach slope and, ξ represents the water surface displacement. The second, third, fourth, and fifth terms of Eq. (1) correspond to linear advection, shoaling effects, nonlinear modulation, and dispersive modulation, respectively. The

depth-dependent coefficients collectively represent the impact of varying bathymetry on wave speed, amplitude, waveform, and stability. The equation is particularly effective for modeling the transformation of nonlinear waves, including tsunamis and internal waves, as they propagate across uneven seabeds. Also, the mSKdV equation is crucial in shallow water dynamics because it effectively describes the behavior of long, nonlinear, and dispersive waves. Its significance lies in its ability to account for nonlinear phenomena such as wave steepening and the development of solitary waves (solitons), as well as the effects of dispersion, where waves of different wavelengths propagate at distinct speeds. This makes the equation vital for applications in fields like coastal engineering, tsunami forecasting, and environmental wave analysis. Solutions to the mSKdV equation are typically obtained using techniques such as Fourier transforms, which convert the equation into an ordinary differential equation in the spectral domain, followed by an inverse transform to interpret the results in the physical domain. While numerical methods can be employed to address more complex scenarios and [25] derived a variable-coefficient Korteweg–de Vries (KdV) equation using the reductive perturbation method to model weakly nonlinear wave propagation over slowly varying water depth, and numerically investigated the influence of bottom topography on wave amplitude and width. However, to date, no analytical techniques have been successfully applied to obtain exact solutions for this class of equations.

That is why to determine its exact solution, this study reviewed various analytical methods, including the generalized $\left(G'/G\right)$ technique [26], the exp $\{-\varphi(\xi)\}$ method [27], the tanh–function method [28], multiple exp-function method [29], the tanh–coth method [30], the modified simple equation technique [31], the Sardar subequation method [32], the modified expansion function method [33], the extended Jacobi elliptic function method [34], the functional variable method [35], the improved Sardar subequation method [36], the generalized Kudryshov method [37], the $\frac{G'}{G'+G+A}$ method [38], Hirota bilinear approach [39] and many others.

Among various techniques, the $\left(\frac{G'}{G}, \frac{1}{G}\right)$ method uses two variables and provides a comprehensive framework for examining different transformations and solution strategies. This adaptability allows it to incorporate trigonometric, hyperbolic, and rational solutions, making it a powerful tool for effectively solving nonlinear equations and achieving meaningful outcomes. Furthermore, the $\left(\frac{G'}{G}, \frac{1}{G}\right)$ expansion method stands out as a significant analytical technique for addressing nonlinear PDEs. By revealing soliton solutions and other behaviors, these methods offer valuable insights into wave interactions and stability, thereby establishing a foundation for further research across various scientific and engineering fields [40–43]. On the other hand, the unified method is an analytical approach that enables the identification of exact solutions for nonlinear PDEs by combining multiple mathematical strategies within a single framework. Its importance stems from its versatility and efficiency, allowing it to be applied to a wide range of nonlinear equations without the need to create new methods for each specific case. This approach not only speeds up the solution process but also deepens the understanding of nonlinear dynamics and their connection to physical phenomena [44, 45]. A brief overview along with the advantages and drawbacks of these methods is provided in Table 1.

After reviewing various methods and recognizing the significance of Eq. (1), this study aims to derive exact solutions for the given nonlinear equation using the aforementioned techniques. The manuscript is structured as follows:

(i) Section 2 offers a brief overview of the methodologies employed in this study.
(ii) Section 3 describes the application of these methodologies in deriving the solutions.

Table 1 (G'/G, 1/G) Method, and Unified Method side by side

Aspect	(G'/G, 1/G) Method	Unified Method
Simplicity	High – straightforward algebraic steps	Moderate – involves more symbolic manipulation
Generality of Solutions	Limited – mostly hyperbolic, trigonometric, exponential	Broader – includes solitons, periodic, and rational
Algebraic Complexity	Low – compact calculations	Higher – more parameters and case handling
Need for Traveling Wave Ansatz	Yes – ODE reduction is essential	Yes – usually starts from ansatz but allows more flexibility
Handling Variable Coefficients	Poor – requires assumptions or approximations	Better – can sometimes accommodate with modifications
Computational Efficiency	Fast and easy to implement	Slower due to parameter analysis
Solution Diversity	Narrow – may miss nonstandard or complex solutions	Wide – supports multiple solution forms
Ideal for	Solitons, periodic waves in constant-coefficient PDEs	Solitons, rational solutions, more general PDEs
Main Drawback	Cannot capture full solution space; oversimplifies	Algebraically intensive; still depends on ansatz

(iii) Section 4 performs a bifurcation analysis.
(iv) Section 5 presents dynamic representations, highlighting various soliton solutions through 3D, 2D, and density plots, along with in-depth discussions.
(v) Section 6 concludes the study with overall insights.
(vi) Finally, the bibliography of references is provided.

2 Methodology's

2.1 The $\left(\frac{G'}{G}, \frac{1}{G}\right)$- Expansion Method

This section explores the $\left(\frac{G'}{G}, \frac{1}{G}\right)$ - expansion method, this method converts nonlinear PDEs into ordinary differential equations (ODEs) by introducing a transformation variable, as outlined in Eq. (3). By substituting the transformation variable into the original nonlinear PDE, the complexity of the problem is significantly reduced. This transformation leverages the inherent symmetries and properties of the PDE to facilitate its conversion into an ODE. The linear ODE obtained through this method is more tractable and allows for a more straightforward analysis and solution. Through the process of rationalizing the analytical procedure, this approach simplifies the problem and produces a linear ODE (see Eq. (5)) [46, 47]. The general form of a nonlinear PDE can be expressed as follows:

$$J\left(\xi, \xi_x, \xi_{xx}, \xi_{xxx}, \xi_t, \xi_{tt}, \xi_{ttt} \ldots \ldots \ldots .\right) = 0 \tag{2}$$

where J is a polynomial.

Considering a transformation variable,θ which converts Eq. (3) into the ODE form, as follows:

$$\xi(x,t) = V(\theta), \theta = (x + \varpi t) \tag{3}$$

Subsequently, Eq. (1) switched to the subsequent polynomial (L is the new form of the previous polynomial):

$$L\left(V, V', V'', V''', \ldots \ldots \ldots, \ldots \ldots \ldots .\right) = 0. \tag{4}$$

The liner ODE described by this methodology can be expressed as follows:

$$G''(\theta) + \wp G(\theta) = \eta \tag{5}$$

subject to:

$$\left.\begin{array}{l} \mathcal{R}_1(\theta) = \frac{G'(\theta)}{G(\theta)} \\ \mathcal{R}_2(\theta) = \frac{1}{G(\theta)} \end{array}\right\}, \tag{6}$$

subsequent in:

$$\left.\begin{array}{l} \mathcal{R}_1' = -\mathcal{R}_1^2 + \eta \mathcal{R}_2 - \wp \\ \mathcal{R}_2' = -\mathcal{R}_1 \times \mathcal{R}_2 \end{array}\right\} \tag{7}$$

Varying on $\wp$, this technique supplies the subsequent cases of solutions:

Case I. When $\wp > 0$:

$$G(\theta) = m_1 sin\left(\theta\sqrt{\wp}\right) + m_2 cos\left(\theta\sqrt{\wp}\right) + {}^{\eta}\!/_{\wp} \tag{8}$$

which produces:

$$\mathcal{R}_2^2 = \left(\frac{\mathcal{R}_1^2 - 2\eta\mathcal{R}_2 + \wp}{\mathbb{C}_1\wp^2 - \eta^2}\right)\wp$$

where

$$\mathbb{C}_1 = m_1^2 + m_2^2$$

Case II. When $\wp < 0$:

$$G(\theta) = m_1 sinh\left(\theta\sqrt{-\wp}\right) + m_2 cosh\left(\theta\sqrt{-\wp}\right) + {}^{\eta}\!/_{\wp} \tag{9}$$

subsequent in:

$$\mathcal{R}_2^2 = -\wp\left(\frac{\mathcal{R}_1^2 - 2\eta\mathcal{R}_2 + \wp}{\mathbb{C}_2\wp^2 + \eta^2}\right)$$

where

$$\mathbb{C}_2 = m_1^2 - m_2^2$$

Case III. When $\wp = 0$:

$$G(\theta) = \frac{\eta\theta^2}{2} + m_1\theta + m_2 \tag{10}$$

which yields:

$$\mathcal{R}_2^2 = \left(\frac{\mathcal{R}_1^2 - 2\eta\mathcal{R}_2}{m_1^2 - 2\eta m_2}\right)$$

The method provides the following general solutions:

$$G(\theta) = \sum_{j=0}^{p} c_j\mathcal{R}_1^j(\theta) + \sum_{j=1}^{P} d_j\mathcal{R}_1^{j-1}(\theta)\mathcal{R}_2(\theta) \tag{11}$$

where c_j, and d_j (j=1, 2, 3,…, p) are the unknown coefficients, assuring that $c_p^2 + d_p^2 \neq 0$, and p represents the balance number.

2.1.1 Method's Workflow

To derive the exact solution of Eq. (1), we start by applying the homogeneous balance method to the transformed equation (such as Eq. (4)) to find the balance number. This balance number is then incorporated into Eq. (11) along with Eqs. (6) and (7), which yield a polynomial of the transformed equation. By setting the coefficients of each term to zero

according to their respective powers in the polynomial, we generate a system of algebraic equations. Solving these equations provides the values of the unknown coefficients. These coefficients are then substituted back into Eq. (11), allowing us to obtain soliton solutions for Eq. (1) expressed in trigonometric functions (as shown in Eq. (8)), hyperbolic functions (as in Eq. (9)), and rational functions (as given by Eq. (10)).

2.2 The Unified Method

The unified method for solving nonlinear PDEs is an all-encompassing approach that simplifies complex nonlinear PDEs into more manageable forms, such as ODEs. This method is highly adaptable and can be used to address a wide variety of nonlinear PDEs, making it a valuable tool in the fields of mathematical physics and applied mathematics. The general solution of this method is defined as follows [48]:

$$V(\theta) = g_0 + \sum_{i=1}^{p} \left\{ g_i f^i + l_i f^{-i} \right\} \tag{12}$$

subject to:

$$f' = f^2 + q \tag{13}$$

where $f' = \frac{df}{d\theta}$; and g_i, l_i (i=1, 2, 3,…, p) are the unknown coefficients with balance number p.

Depending on the values of q, Eq. (13) yields the following solution cases:

Case I: When $\boldsymbol{q} < 0$:

$$f = \frac{\sqrt{-q\left(\alpha^2 + \beta^2\right)} - \alpha\sqrt{-q}cosh\left\{2\sqrt{-q}(\theta + \delta)\right\}}{\alpha sinh\left\{2\sqrt{-q}(\theta + \delta)\right\} + \beta} \tag{14}$$

$$f = \frac{-\sqrt{-q\left(\alpha^2 + \beta^2\right)} - \alpha\sqrt{-q}cosh\left\{2\sqrt{-q}(\theta + \delta)\right\}}{\alpha sinh\left\{2\sqrt{-q}(\theta + \delta)\right\} + \beta} \tag{15}$$

$$f = \frac{-2\alpha\sqrt{-q}}{\alpha + cosh\left\{2\sqrt{-q}(\theta + \delta)\right\} - sinh\left\{2\sqrt{-q}(\theta + \delta)\right\}} + \sqrt{-q} \tag{16}$$

$$f = \frac{2\alpha\sqrt{-q}}{\alpha + cosh\left\{2\sqrt{-q}(\theta + \delta)\right\} + sinh\left\{2\sqrt{-q}(\theta + \delta)\right\}} - \sqrt{-q} \tag{17}$$

Case II: When $\boldsymbol{q} > 0$:

$$f = \frac{\sqrt{q\left(\alpha^2 - \beta^2\right)} - \alpha\sqrt{q}cos\left\{2\sqrt{q}(\theta + \delta)\right\}}{\alpha sin\left\{2\sqrt{q}(\theta + \delta)\right\} + \beta} \tag{18}$$

$$f = \frac{-\sqrt{q(\alpha^2 - \beta^2)} - \alpha\sqrt{q}cos\{2\sqrt{q}(\theta + \delta)\}}{\alpha sin\{2\sqrt{q}(\theta + \delta)\} + \beta} \tag{19}$$

$$f = \frac{-2i\alpha\sqrt{q}}{\alpha + cos\{2\sqrt{q}(\theta + \delta)\} - isin\{2\sqrt{q}(\theta + \delta)\}} + i\sqrt{q} \tag{20}$$

$$f = \frac{2i\alpha\sqrt{q}}{\alpha + cos\{2\sqrt{q}(\theta + \delta)\} + isin\{2\sqrt{q}(\theta + \delta)\}} - i\sqrt{q} \tag{21}$$

Case III: When $\boldsymbol{q} = 0$:

$$f = -\frac{1}{(\theta + \delta)} \tag{22}$$

In all cases, α and β are real arbitrary constants, δ is an arbitrary constant, and i is the imaginary unit.

2.2.1 Method Workflow

A text-based representation of a flowchart for the unified method workflow for solving nonlinear PDEs is presented in Flowchart 1.

3 Method's Application

3.1 Transformed to ODE

The equation is transformed into an ODE by using the transformation method outlined in Section 2, which leads to:

$$\frac{\gamma^2 h^{\frac{5}{2}}}{6} V''' + \left(\sqrt{h} + \frac{3\varepsilon}{2\sqrt{h}} V + \varpi\right) V' + \frac{h_x}{4\sqrt{h}} V = 0 \tag{23}$$

The second term on the left-hand side of Eq. (23) represents shoaling according to Green's law and can be expressed for linear waves as $\sqrt{h}V' = -\frac{h_x}{4\sqrt{h}} V$ [49], thus, after integrating once and setting the arbitrary constant to zero, Eq. (23) transforms to:

$$\frac{\gamma^2 h^{\frac{5}{2}}}{6} V'' + \left(\frac{3\varepsilon}{4\sqrt{h}}\right) V^2 + \varpi V = 0 \tag{24}$$

Next, we applied the above-mentioned methodologies to extract the exact solution of this equation for uniform sloping beach.

3.2 The $\left(\frac{G'}{G}, \frac{1}{G}\right)$- Expansion Method

By applying the homogeneous balance method to Eq. (24), we derive: $p = 2$, that yields the following general solution:

$$V(\theta) = c_0 + c_1\mathcal{R}_1(\theta) + d_1\mathcal{R}_2(\theta) + c_2\mathcal{R}_1^2(\theta) + d_2\mathcal{R}_1(\theta)\mathcal{R}_2(\theta) \tag{25}$$

For $\wp > 0$:

Using the described methodology, we identified a series of algebraic equations. Solving these equations provided the values for the unknown coefficients:

Set 1:

$$\left.\begin{aligned} c_0 &= -\frac{2\left(\sqrt{h}\right)^6\gamma^2\wp}{3\epsilon} \\ c_1 &= 0 \\ c_2 &= -\frac{2\left(\sqrt{h}\right)^6\gamma^2}{3\epsilon} \\ d_1 &= \frac{2\left(\sqrt{h}\right)^6\gamma^2\eta}{3\epsilon} \\ d_2 &= \pm\frac{2\left(\sqrt{h}\right)^6\gamma^2\sqrt{\mathbb{C}_1\wp^2-\eta^2}}{3\epsilon\sqrt{\wp}} \\ \varpi &= \frac{1}{6}\left(\sqrt{h}\right)^5\gamma^2\wp \end{aligned}\right\} \tag{26}$$

Inserting these values into Eq. (25), then into Eq. (3), and finally Eq. (1) produces the following general solution:

$$\begin{aligned} \xi(x,t) = -\frac{2\left(\sqrt{h}\right)^6\gamma^2\wp}{3\epsilon} + \frac{2\left(\sqrt{h}\right)^6\gamma^2\eta}{3\epsilon}\frac{1}{m_1 sin(\theta\sqrt{\wp}) + m_2 cos(\theta\sqrt{\wp}) + {}^{\eta}/_{\wp}} - \\ \frac{2\left(\sqrt{h}\right)^6\gamma^2}{3\epsilon}\wp\left\{\frac{m_1 cos(\theta\sqrt{\wp}) - m_2 sin(\theta\sqrt{\wp})}{m_1 sin(\theta\sqrt{\wp}) + m_2 cos(\theta\sqrt{\wp}) + {}^{\eta}/_{\wp}}\right\}^2 \pm \\ \frac{2\left(\sqrt{h}\right)^6\gamma^2\sqrt{\mathbb{C}_1\wp^2-\eta^2}}{3\epsilon}\frac{m_1 cos(\theta\sqrt{\wp}) - m_2 sin(\theta\sqrt{\wp})}{\left\{m_1 sin(\theta\sqrt{\wp}) + m_2 cos(\theta\sqrt{\wp}) + {}^{\eta}/_{\wp}\right\}^2} \end{aligned} \tag{27}$$

If $\eta = 0$, and $m_2 = 0$ but $m_1 \neq 0$, Eq. (27) yields:

$$\xi(x,t) = -\frac{2\left(\sqrt{h}\right)^6\gamma^2\wp}{3\epsilon} - \frac{2\left(\sqrt{h}\right)^6\gamma^2}{3\epsilon}\wp\left\{cot\left(\theta\sqrt{\wp}\right)\right\}^2 \pm \frac{2\left(\sqrt{h}\right)^6\gamma^2\wp}{3\epsilon}cot\left(\theta\sqrt{\wp}\right)cosec\left(\theta\sqrt{\wp}\right) \tag{28}$$

Similarly, if $\eta = 0$, and $m_1 = 0$ but $m_2 \neq 0$, Eq. (27) yields:

$$\xi(x,t) = -\frac{2\left(\sqrt{h}\right)^6\gamma^2\wp}{3\epsilon} - \frac{2\left(\sqrt{h}\right)^6\gamma^2}{3\epsilon}\wp\left\{tan(\theta\sqrt{(\wp)}\right\}^2 \pm \frac{2\left(\sqrt{h}\right)^6\gamma^2\wp}{3\epsilon}tan\left(\theta\sqrt{\wp}\right)sec\left(\theta\sqrt{\wp}\right) \tag{29}$$

where

Flowchart 1 Workflow of unified method

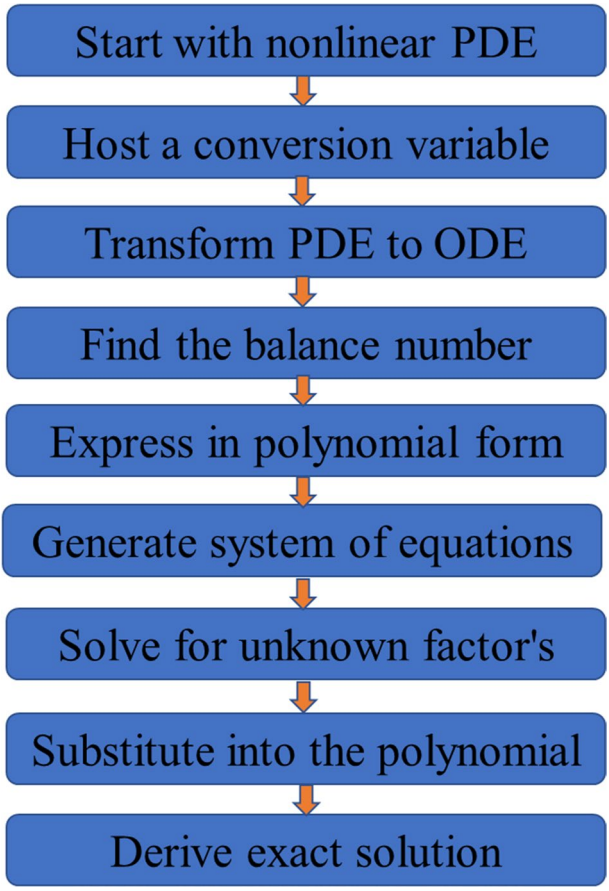

$$\theta = (x + \varpi t)$$

Set 2:

$$\left.\begin{aligned} c_0 &= -\frac{4\left(\sqrt{h}\right)^6 \gamma^2 \wp}{9\epsilon} \\ c_1 &= 0 \\ c_2 &= -\frac{2\left(\sqrt{h}\right)^6 \gamma^2}{3\epsilon} \\ d_1 &= \frac{2\left(\sqrt{h}\right)^6 \gamma^2 \eta}{3\epsilon} \\ d_2 &= \pm\frac{2\left(\sqrt{h}\right)^6 \gamma^2 \sqrt{\mathbb{C}_1 \wp^2 - \eta^2}}{3\epsilon\sqrt{\wp}} \\ \varpi &= -\frac{1}{6}\left(\sqrt{h}\right)^5 \gamma^2 \wp \end{aligned}\right\} \tag{30}$$

By inserting these values into Eq. (25), followed by Eq. (3), and ultimately Eq. (1), we obtain the following general solution:

$$\xi(x,t) = -\frac{4\left(\sqrt{h}\right)^6\gamma^2\wp}{9\epsilon} + \frac{2\left(\sqrt{h}\right)^6\gamma^2\eta}{3\epsilon}\frac{1}{m_1 sin\left(\theta\sqrt{\wp}\right) + m_2 cos\left(\theta\sqrt{\wp}\right) + {}^{\eta}/_{\wp}} - \frac{2\left(\sqrt{h}\right)^6\gamma^2}{3\epsilon}\wp\left\{\frac{m_1 cos\left(\theta\sqrt{\wp}\right) - m_2 sin\left(\theta\sqrt{\wp}\right)}{m_1 sin\left(\theta\sqrt{\wp}\right) + m_2 cos\left(\theta\sqrt{\wp}\right) + {}^{\eta}/_{\wp}}\right\}^2 \pm \frac{2\left(\sqrt{h}\right)^6\gamma^2\sqrt{\mathbb{C}_1\wp^2 - \eta^2}}{3\epsilon}\frac{m_1 cos\left(\theta\sqrt{\wp}\right) - m_2 sin\left(\theta\sqrt{\wp}\right)}{\left\{m_1 sin\left(\theta\sqrt{\wp}\right) + m_2 cos\left(\theta\sqrt{\wp}\right) + {}^{\eta}/_{\wp}\right\}^2} \tag{31}$$

If $\eta = 0$, and $m_2 = 0$ but $m_1 \neq 0$, Eq. (31) yields:

$$\xi(x,t) = -\frac{4\left(\sqrt{h}\right)^6\gamma^2\wp}{9\epsilon} - \frac{2\left(\sqrt{h}\right)^6\gamma^2}{3\epsilon}\wp\left\{cot\left(\theta\sqrt{\wp}\right)\right\}^2 \pm \frac{2\left(\sqrt{h}\right)^6\gamma^2\wp}{3\epsilon}cot\left(\theta\sqrt{\wp}\right)cosec\left(\theta\sqrt{\wp}\right) \tag{32}$$

Likewise, if $\eta = 0$, and $m_1 = 0$ but $m_2 \neq 0$, Eq. (31) yields:

$$\xi(x,t) = -\frac{4\left(\sqrt{h}\right)^6\gamma^2\wp}{9\epsilon} - \frac{2\left(\sqrt{h}\right)^6\gamma^2}{3\epsilon}\wp\left\{tan(\theta\sqrt{(\wp)}\right\}^2 \pm \frac{2\left(\sqrt{h}\right)^6\gamma^2\wp}{3\epsilon}tan\left(\theta\sqrt{\wp}\right)sec\left(\theta\sqrt{\wp}\right) \tag{33}$$

where

$$\theta = (x + \varpi t)$$

For $\wp < 0$:
Similarly, in this case, the following unknown coefficients are obtained:
Set 1:

$$\left.\begin{aligned} c_0 &= -\frac{2\left(\sqrt{h}\right)^6\gamma^2\wp}{3\epsilon} \\ c_1 &= 0 \\ c_2 &= -\frac{2\left(\sqrt{h}\right)^6\gamma^2}{3\epsilon} \\ d_1 &= \frac{2\left(\sqrt{h}\right)^6\gamma^2\eta}{3\epsilon} \\ d_2 &= \pm\frac{2\left(\sqrt{h}\right)^6\gamma^2\sqrt{\mathbb{C}_2\wp^2+\eta^2}}{3\epsilon\sqrt{-\wp}} \\ \varpi &= \frac{1}{6}\left(\sqrt{h}\right)^5\gamma^2\wp \end{aligned}\right\} \tag{34}$$

Substituting these values into Eq. (25), followed by Eq. (3), and finally into Eq. (1), results in the following general solution:

$$\xi(x,t) = -\frac{2\left(\sqrt{h}\right)^6\gamma^2\wp}{3\epsilon} + \frac{2\left(\sqrt{h}\right)^6\gamma^2\eta}{3\epsilon}\frac{1}{m_1 sinh\left(\theta\sqrt{-\wp}\right) + m_2 cosh\left(\theta\sqrt{-\wp}\right) + {}^{\eta}/_{\wp}} + \frac{2\left(\sqrt{h}\right)^6\gamma^2}{3\epsilon}\wp\left\{\frac{m_1 cosh\left(\theta\sqrt{-\wp}\right) + m_2 sinh\left(\theta\sqrt{-\wp}\right)}{m_1 sinh\left(\theta\sqrt{-\wp}\right) + m_2 cosh\left(\theta\sqrt{-\wp}\right) + {}^{\eta}/_{\wp}}\right\}^2 \pm \frac{2\left(\sqrt{h}\right)^6\gamma^2\sqrt{\mathbb{C}_2\wp^2+\eta^2}}{3\epsilon}\frac{m_1 cosh\left(\theta\sqrt{-\wp}\right) + m_2 sinh\left(\theta\sqrt{-\wp}\right)}{\left\{m_1 sinh\left(\theta\sqrt{-\wp}\right) + m_2 cosh\left(\theta\sqrt{-\wp}\right) + {}^{\eta}/_{\wp}\right\}^2} \tag{35}$$

where

$$\theta = (x + \varpi t)$$

If both $\eta = m_2 = 0$ but $m_1 \neq 0$, Eq. (35) gives:

$$\xi(x,t) = -\frac{2\left(\sqrt{h}\right)^6\gamma^2\wp}{3\epsilon} + \frac{2\left(\sqrt{h}\right)^6\gamma^2}{3\epsilon}\wp\left\{coth\left(\theta\sqrt{-\wp}\right)\right\}^2 \pm \frac{2\left(\sqrt{h}\right)^6\gamma^2\wp}{3\epsilon}coth\left(\theta\sqrt{-\wp}\right)cosech\left(\theta\sqrt{-\wp}\right) \tag{36}$$

where $\theta = (x + \varpi t)$.

Set 2:

$$\left.\begin{aligned} c_0 &= -\frac{4\left(\sqrt{h}\right)^6\gamma^2\wp}{9\epsilon} \\ c_1 &= 0 \\ c_2 &= -\frac{2\left(\sqrt{h}\right)^6\gamma^2}{3\epsilon} \\ d_1 &= \frac{2\left(\sqrt{h}\right)^6\gamma^2\eta}{3\epsilon} \\ d_2 &= \pm\frac{2\left(\sqrt{h}\right)^6\gamma^2\sqrt{\mathbb{C}_2\wp^2+\eta^2}}{3\epsilon\sqrt{-\wp}} \\ \varpi &= -\frac{1}{6}\left(\sqrt{h}\right)^5\gamma^2\wp \end{aligned}\right\} \tag{37}$$

By substituting these values into Eq. (25), then into Eq. (3), and finally into Eq. (1), we obtain the following general solution:

$$\xi(x,t) = -\frac{4\left(\sqrt{h}\right)^6\gamma^2\wp}{9\epsilon} + \frac{2\left(\sqrt{h}\right)^6\gamma^2\eta}{3\epsilon}\frac{1}{m_1 sinh\left(\theta\sqrt{-\wp}\right) + m_2 cosh\left(\theta\sqrt{-\wp}\right) + {}^{\eta}/_{\wp}} + \frac{2\left(\sqrt{h}\right)^6\gamma^2}{3\epsilon}\wp\left\{\frac{m_1 cosh\left(\theta\sqrt{-\wp}\right) + m_2 sinh\left(\theta\sqrt{-\wp}\right)}{m_1 sinh\left(\theta\sqrt{-\wp}\right) + m_2 cosh\left(\theta\sqrt{-\wp}\right) + {}^{\eta}/_{\wp}}\right\}^2 \pm \frac{2\left(\sqrt{h}\right)^6\gamma^2\sqrt{\mathbb{C}_2\wp^2+\eta^2}}{3\epsilon}\frac{m_1 cosh\left(\theta\sqrt{-\wp}\right) + m_2 sinh\left(\theta\sqrt{-\wp}\right)}{\left\{m_1 sinh\left(\theta\sqrt{-\wp}\right) + m_2 cosh\left(\theta\sqrt{-\wp}\right) + {}^{\eta}/_{\wp}\right\}^2} \tag{38}$$

If both $\eta = m_2 = 0$ but $m_1 \neq 0$, Eq. (38) gives:

$$\xi(x,t) = -\frac{4\left(\sqrt{h}\right)^6\gamma^2\wp}{9\epsilon} + \frac{2\left(\sqrt{h}\right)^6\gamma^2}{3\epsilon}\wp\left\{coth\left(\theta\sqrt{-\wp}\right)\right\}^2 \pm \frac{2\left(\sqrt{h}\right)^6\gamma^2\wp}{3\epsilon}coth\left(\theta\sqrt{-\wp}\right)cosech\left(\theta\sqrt{-\wp}\right) \tag{39}$$

where

$$\theta = (x + \varpi t)$$

For $\wp = 0$:
Similarly, in this case there is no feasible solution.

3.3 The Unified Method

Similarly, since we derive: $p = 2$, that yields the following general solution for this method:

$$V(\theta) = g_0 + g_1 f + g_2 f^2 + l_1 f^{-1} + l_2 f^{-2} \tag{40}$$

Following the outlined methodology, we derived a set of algebraic equations. Solving these equations provided the values for the unknown coefficients as follows:

Set 1:

$$\left.\begin{array}{l} g_0 = -\frac{8\left(\sqrt{h}\right)^6 q\gamma^2}{3\epsilon} \\ g_1 = 0 \\ g_2 = -\frac{4\left(\sqrt{h}\right)^6\gamma^2}{3\epsilon} \\ l_1 = 0 \\ l_2 = -\frac{4\left(\sqrt{h}\right)^6 q^2\gamma^2}{3\epsilon} \\ \varpi = \frac{8}{3}\left(\sqrt{h}\right)^5 q\gamma^2 \end{array}\right\} \tag{41}$$

Inserting these values into Eq. (25), then into Eq. (3), and finally Eq. (1) produces the following general solution:

Case I: When $q < 0$:

$$\begin{aligned}\xi_1(x,t) = -\frac{8\left(\sqrt{h}\right)^6 q\gamma^2}{3\epsilon} - \frac{4\left(\sqrt{h}\right)^6\gamma^2}{3\epsilon}\left[\frac{\sqrt{-q\left(\alpha^2+\beta^2\right)} - \alpha\sqrt{-q}cosh\left\{2\sqrt{-q}(\theta+\delta)\right\}}{\alpha sinh\left\{2\sqrt{-q}(\theta+\delta)\right\} + \beta}\right]^2 \\ -\frac{4\left(\sqrt{h}\right)^6 q^2\gamma^2}{3\epsilon}\left[\frac{\alpha sinh\left\{2\sqrt{-q}(\theta+\delta)\right\} + \beta}{\sqrt{-q\left(\alpha^2+\beta^2\right)} - \alpha\sqrt{-q}cosh\left\{2\sqrt{-q}(\theta+\delta)\right\}}\right]^2\end{aligned} \tag{42}$$

$$\xi_2(x,t) = -\frac{8\left(\sqrt{h}\right)^6 q\gamma^2}{3\epsilon} - \frac{4\left(\sqrt{h}\right)^6 \gamma^2}{3\epsilon}\left[\frac{-\sqrt{-q(\alpha^2+\beta^2)} - \alpha\sqrt{-q}cosh\{2\sqrt{-q}(\theta+\delta)\}}{\alpha sinh\{2\sqrt{-q}(\theta+\delta)\}+\beta}\right]^2 - \frac{4\left(\sqrt{h}\right)^6 q^2\gamma^2}{3\epsilon}\left[\frac{\alpha sinh\{2\sqrt{-q}(\theta+\delta)\}+\beta}{-\sqrt{-q(\alpha^2+\beta^2)} - \alpha\sqrt{-q}cosh\{2\sqrt{-q}(\theta+\delta)\}}\right]^2 \tag{43}$$

$$\xi_3(x,t) = -\frac{8\left(\sqrt{h}\right)^6 q\gamma^2}{3\epsilon} - \frac{4\left(\sqrt{h}\right)^6 \gamma^2}{3\epsilon}\left[\frac{-2\alpha\sqrt{-q}}{\alpha + cosh\{2\sqrt{-q}(\theta+\delta)\} - sinh\{2\sqrt{-q}(\theta+\delta)\}} + \sqrt{-q}\right]^2 - \frac{4\left(\sqrt{h}\right)^6 q^2\gamma^2}{3\epsilon}\left[\frac{\alpha + cosh\{2\sqrt{-q}(\theta+\delta)\} - sinh\{2\sqrt{-q}(\theta+\delta)\}}{-\alpha + cosh\{2\sqrt{-q}(\theta+\delta)\} - sinh\{2\sqrt{-q}(\theta+\delta)\}}\right]^2 \tag{44}$$

$$\xi_4(x,t) = -\frac{8\left(\sqrt{h}\right)^6 q\gamma^2}{3\epsilon} - \frac{4\left(\sqrt{h}\right)^6 \gamma^2}{3\epsilon}\left[\frac{2\alpha\sqrt{-q}}{\alpha + cosh\{2\sqrt{-q}(\theta+\delta)\} + sinh\{2\sqrt{-q}(\theta+\delta)\}} - \sqrt{-q}\right]^2 - \frac{4\left(\sqrt{h}\right)^6 q^2\gamma^2}{3\epsilon}\left[\frac{\alpha + cosh\{2\sqrt{-q}(\theta+\delta)\} + sinh\{2\sqrt{-q}(\theta+\delta)\}}{\alpha - cosh\{2\sqrt{-q}(\theta+\delta)\} - sinh\{2\sqrt{-q}(\theta+\delta)\}}\right]^2 \tag{45}$$

Case II: When $\boldsymbol{q} > 0$:

$$\xi_5(x,t) = -\frac{8\left(\sqrt{h}\right)^6 q\gamma^2}{3\epsilon} - \frac{4\left(\sqrt{h}\right)^6 \gamma^2}{3\epsilon}\left[\frac{\sqrt{q(\alpha^2-\beta^2)} - \alpha\sqrt{q}cos\{2\sqrt{q}(\theta+\delta)\}}{\alpha sin\{2\sqrt{q}(\theta+\delta)\}+\beta}\right]^2 - \frac{4\left(\sqrt{h}\right)^6 q^2\gamma^2}{3\epsilon}\left[\frac{\alpha sin\{2\sqrt{q}(\theta+\delta)\}+\beta}{\sqrt{q(\alpha^2-\beta^2)} - \alpha\sqrt{q}cos\{2\sqrt{q}(\theta+\delta)\}}\right]^2 \tag{46}$$

$$\xi_6(x,t) = -\frac{8\left(\sqrt{h}\right)^6 q\gamma^2}{3\epsilon} - \frac{4\left(\sqrt{h}\right)^6 \gamma^2}{3\epsilon}\left[\frac{-\sqrt{q(\alpha^2-\beta^2)} - \alpha\sqrt{q}cos\{2\sqrt{q}(\theta+\delta)\}}{\alpha sin\{2\sqrt{q}(\theta+\delta)\}+\beta}\right]^2 - \frac{4\left(\sqrt{h}\right)^6 q^2\gamma^2}{3\epsilon}\left[\frac{\alpha sin\{2\sqrt{q}(\theta+\delta)\}+\beta}{-\sqrt{q(\alpha^2-\beta^2)} - \alpha\sqrt{q}cos\{2\sqrt{q}(\theta+\delta)\}}\right]^2 \tag{47}$$

$$\xi_7(x,t) = -\frac{8\left(\sqrt{h}\right)^6 q\gamma^2}{3\epsilon} - \frac{4\left(\sqrt{h}\right)^6 \gamma^2}{3\epsilon}\left[\frac{-2i\alpha\sqrt{q}}{\alpha + cos\{2\sqrt{q}(\theta+\delta)\} - isin\{2\sqrt{q}(\theta+\delta)\}} + i\sqrt{q}\right]^2 + \frac{4\left(\sqrt{h}\right)^6 q^2\gamma^2}{3\epsilon}\left[\frac{\alpha + cos\{2\sqrt{q}(\theta+\delta)\} - isin\{2\sqrt{q}(\theta+\delta)\}}{-\alpha + cos\{2\sqrt{q}(\theta+\delta)\} - isin\{2\sqrt{q}(\theta+\delta)\}}\right]^2 \tag{48}$$

$$\xi_8(x,t) = -\frac{8\left(\sqrt{h}\right)^6 q\gamma^2}{3\epsilon} - \frac{4\left(\sqrt{h}\right)^6 \gamma^2}{3\epsilon}\left[\frac{2i\alpha\sqrt{q}}{\alpha + cos\{2\sqrt{q}(\theta+\delta)\} + isin\{2\sqrt{q}(\theta+\delta)\}} - i\sqrt{q}\right]^2 + \frac{4\left(\sqrt{h}\right)^6 q^2\gamma^2}{3\epsilon}\left[\frac{\alpha + cos\{2\sqrt{q}(\theta+\delta)\} + isin\{2\sqrt{q}(\theta+\delta)\}}{\alpha - cos\{2\sqrt{q}(\theta+\delta)\} - isin\{2\sqrt{q}(\theta+\delta)\}}\right]^2 \tag{49}$$

Case III: When $q = 0$:

$$\xi_9(x,t) = -\frac{4\left(\sqrt{h}\right)^6 \gamma^2}{3\epsilon}\frac{1}{(\theta+\delta)^2} \tag{50}$$

Set 2:

$$\left.\begin{aligned} g_0 &= -\frac{4\left(\sqrt{h}\right)^6 q\gamma^2}{3\epsilon} \\ g_1 &= 0 \\ g_2 &= 0 \\ l_1 &= 0 \\ l_2 &= -\frac{4\left(\sqrt{h}\right)^6 q^2\gamma^2}{3\epsilon} \\ \varpi &= \frac{2}{3}\left(\sqrt{h}\right)^5 q\gamma^2 \end{aligned}\right\} \tag{51}$$

Inserting these values into Eq. (25), then into Eq. (3), and finally Eq. (1) produces the following general solution:

Case I: When $q < 0$:

$$\xi_{10}(x,t) = -\frac{4\left(\sqrt{h}\right)^6 q\gamma^2}{3\epsilon} - \frac{4\left(\sqrt{h}\right)^6 q^2\gamma^2}{3\epsilon}\left[\frac{\alpha sinh\{2\sqrt{-q}(\theta+\delta)\} + \beta}{\sqrt{-q(\alpha^2+\beta^2)} - \alpha\sqrt{-q}cosh\{2\sqrt{-q}(\theta+\delta)\}}\right]^2 \tag{52}$$

$$\xi_{11}(x,t) = -\frac{4\left(\sqrt{h}\right)^6 q\gamma^2}{3\epsilon} - \frac{4\left(\sqrt{h}\right)^6 q^2\gamma^2}{3\epsilon}\left[\frac{\alpha sinh\{2\sqrt{-q}(\theta+\delta)\} + \beta}{-\sqrt{-q(\alpha^2+\beta^2)} - \alpha\sqrt{-q}cosh\{2\sqrt{-q}(\theta+\delta)\}}\right]^2 \tag{53}$$

$$\xi_{12}(x,t) = -\frac{4\left(\sqrt{h}\right)^6 q\gamma^2}{3\epsilon} - \frac{4\left(\sqrt{h}\right)^6 q^2\gamma^2}{3\epsilon}\left[\frac{\alpha + cosh\{2\sqrt{-q}(\theta+\delta)\} - sinh\{2\sqrt{-q}(\theta+\delta)\}}{-\alpha + cosh\{2\sqrt{-q}(\theta+\delta)\} - sinh\{2\sqrt{-q}(\theta+\delta)\}}\right]^2 \tag{54}$$

$$\xi_{13}(x,t) = -\frac{4\left(\sqrt{h}\right)^6 q\gamma^2}{3\epsilon} - \frac{4\left(\sqrt{h}\right)^6 q^2\gamma^2}{3\epsilon}\left[\frac{\alpha + cosh\{2\sqrt{-q}(\theta+\delta)\} + sinh\{2\sqrt{-q}(\theta+\delta)\}}{\alpha - cosh\{2\sqrt{-q}(\theta+\delta)\} - sinh\{2\sqrt{-q}(\theta+\delta)\}}\right]^2 \tag{55}$$

Case II: When $q > 0$:

$$\xi_{14}(x,t) = -\frac{4\left(\sqrt{h}\right)^6 q\gamma^2}{3\epsilon} - \frac{4\left(\sqrt{h}\right)^6 q^2\gamma^2}{3\epsilon}\left[\frac{\alpha sin\{2\sqrt{q}(\theta+\delta)\}+\beta}{\sqrt{q\left(\alpha^2-\beta^2\right)}-\alpha\sqrt{q}cos\{2\sqrt{q}(\theta+\delta)\}}\right]^2 \tag{56}$$

$$\xi_{15}(x,t) = -\frac{4\left(\sqrt{h}\right)^6 q\gamma^2}{3\epsilon} - \frac{4\left(\sqrt{h}\right)^6 q^2\gamma^2}{3\epsilon}\left[\frac{\alpha sin\{2\sqrt{q}(\theta+\delta)\}+\beta}{-\sqrt{q\left(\alpha^2-\beta^2\right)}-\alpha\sqrt{q}cos\{2\sqrt{q}(\theta+\delta)\}}\right]^2 \tag{57}$$

$$\xi_{16}(x,t) = -\frac{4\left(\sqrt{h}\right)^6 q\gamma^2}{3\epsilon} + \frac{4\left(\sqrt{h}\right)^6 q^2\gamma^2}{3\epsilon}\left[\frac{\alpha+cos\{2\sqrt{q}(\theta+\delta)\}-isin\{2\sqrt{q}(\theta+\delta)\}}{-\alpha+cos\{2\sqrt{q}(\theta+\delta)\}-isin\{2\sqrt{q}(\theta+\delta)\}}\right]^2 \tag{58}$$

$$\xi_{17}(x,t) = -\frac{4\left(\sqrt{h}\right)^6 q\gamma^2}{3\epsilon} + \frac{4\left(\sqrt{h}\right)^6 q^2\gamma^2}{3\epsilon}\left[\frac{\alpha+cos\{2\sqrt{q}(\theta+\delta)\}+isin\{2\sqrt{q}(\theta+\delta)\}}{\alpha-cos\{2\sqrt{q}(\theta+\delta)\}-isin\{2\sqrt{q}(\theta+\delta)\}}\right]^2 \tag{59}$$

Case III: When $q = 0$:

There is no feasible solution for this case.

Set 3:

$$\left.\begin{aligned} g_0 &= -\tfrac{4\left(\sqrt{h}\right)^6 q\gamma^2}{3\epsilon} \\ g_1 &= 0 \\ g_2 &= -\tfrac{4\left(\sqrt{h}\right)^6 \gamma^2}{3\epsilon} \\ l_1 &= 0 \\ l_2 &= 0 \\ \varpi &= \tfrac{2}{3}\left(\sqrt{h}\right)^5 q\gamma^2 \end{aligned}\right\} \tag{60}$$

Inserting these values into Eq. (25), then into Eq. (3), and finally Eq. (1) produces the following general solution:

Case I: When $q < 0$:

$$\xi_{18}(x,t) = -\frac{4\left(\sqrt{h}\right)^6 q\gamma^2}{3\epsilon} - \frac{4\left(\sqrt{h}\right)^6 \gamma^2}{3\epsilon}\left[\frac{\sqrt{-q\left(\alpha^2+\beta^2\right)}-\alpha\sqrt{-q}cosh\{2\sqrt{-q}(\theta+\delta)\}}{\alpha sinh\{2\sqrt{-q}(\theta+\delta)\}+\beta}\right]^2 \tag{61}$$

$$\xi_{19}(x,t) = -\frac{4\left(\sqrt{h}\right)^6 q\gamma^2}{3\epsilon} - \frac{4\left(\sqrt{h}\right)^6 \gamma^2}{3\epsilon}\left[\frac{-\sqrt{-q\left(\alpha^2+\beta^2\right)}-\alpha\sqrt{-q}cosh\{2\sqrt{-q}(\theta+\delta)\}}{\alpha sinh\{2\sqrt{-q}(\theta+\delta)\}+\beta}\right]^2 \tag{62}$$

$$\xi_{20}(x,t) = -\frac{4\left(\sqrt{h}\right)^6 q\gamma^2}{3\epsilon} - \frac{4\left(\sqrt{h}\right)^6 \gamma^2}{3\epsilon}\left[\frac{-2\alpha\sqrt{-q}}{\alpha + cosh\{2\sqrt{-q}(\theta+\delta)\} - sinh\{2\sqrt{-q}(\theta+\delta)\}} + \sqrt{-q}\right]^2 \tag{63}$$

$$\xi_{21}(x,t) = -\frac{4\left(\sqrt{h}\right)^6 q\gamma^2}{3\epsilon} - \frac{4\left(\sqrt{h}\right)^6 \gamma^2}{3\epsilon}\left[\frac{2\alpha\sqrt{-q}}{\alpha + cosh\{2\sqrt{-q}(\theta+\delta)\} + sinh\{2\sqrt{-q}(\theta+\delta)\}} - \sqrt{-q}\right]^2 \tag{64}$$

Case II: When $\boldsymbol{q} > 0$:

$$\xi_{22}(x,t) = -\frac{4\left(\sqrt{h}\right)^6 q\gamma^2}{3\epsilon} - \frac{4\left(\sqrt{h}\right)^6 \gamma^2}{3\epsilon}\left[\frac{\sqrt{q(\alpha^2-\beta^2)} - \alpha\sqrt{q}cos\{2\sqrt{q}(\theta+\delta)\}}{\alpha sin\{2\sqrt{q}(\theta+\delta)\} + \beta}\right]^2 \tag{65}$$

$$\xi_{23}(x,t) = -\frac{4\left(\sqrt{h}\right)^6 q\gamma^2}{3\epsilon} - \frac{4\left(\sqrt{h}\right)^6 \gamma^2}{3\epsilon}\left[\frac{-\sqrt{q(\alpha^2-\beta^2)} - \alpha\sqrt{q}cos\{2\sqrt{q}(\theta+\delta)\}}{\alpha sin\{2\sqrt{q}(\theta+\delta)\} + \beta}\right]^2 \tag{66}$$

$$\xi_{24}(x,t) = -\frac{4\left(\sqrt{h}\right)^6 q\gamma^2}{3\epsilon} - \frac{4\left(\sqrt{h}\right)^6 \gamma^2}{3\epsilon}\left[\frac{-2i\alpha\sqrt{q}}{\alpha + cos\{2\sqrt{q}(\theta+\delta)\} - isin\{2\sqrt{q}(\theta+\delta)\}} + i\sqrt{q}\right]^2 \tag{67}$$

$$\xi_{25}(x,t) = -\frac{4\left(\sqrt{h}\right)^6 q\gamma^2}{3\epsilon} - \frac{4\left(\sqrt{h}\right)^6 \gamma^2}{3\epsilon}\left[\frac{2i\alpha\sqrt{q}}{\alpha + cos\{2\sqrt{q}(\theta+\delta)\} + isin\{2\sqrt{q}(\theta+\delta)\}} - i\sqrt{q}\right]^2 \tag{68}$$

Case III: When $\boldsymbol{q} = 0$:

$$\xi_{26}(x,t) = -\frac{4\left(\sqrt{h}\right)^6 \gamma^2}{3\epsilon}\frac{1}{(\theta+\delta)^2} \tag{69}$$

Eq. (69) is exactly the same as Eq. (50).

Set 4:

$$\left.\begin{aligned} g_0 &= \frac{8\left(\sqrt{h}\right)^6 q\gamma^2}{9\epsilon} \\ g_1 &= 0 \\ g_2 &= -\frac{4\left(\sqrt{h}\right)^6 \gamma^2}{3\epsilon} \\ l_1 &= 0 \\ l_2 &= -\frac{4\left(\sqrt{h}\right)^6 q^2\gamma^2}{3\epsilon} \\ \varpi &= -\frac{8}{3}\left(\sqrt{h}\right)^5 q\gamma^2 \end{aligned}\right\} \tag{70}$$

Case I: When $q < 0$:

$$\xi_{27}(x,t) = \frac{8\left(\sqrt{h}\right)^6 q\gamma^2}{9\epsilon} - \frac{4\left(\sqrt{h}\right)^6 \gamma^2}{3\epsilon}\left[\frac{\sqrt{-q\left(\alpha^2+\beta^2\right)} - \alpha\sqrt{-q}cosh\left\{2\sqrt{-q}(\theta+\delta)\right\}}{\alpha sinh\left\{2\sqrt{-q}(\theta+\delta)\right\}+\beta}\right]^2 - \frac{4\left(\sqrt{h}\right)^6 q^2\gamma^2}{3\epsilon}\left[\frac{\alpha sinh\left\{2\sqrt{-q}(\theta+\delta)\right\}+\beta}{\sqrt{-q\left(\alpha^2+\beta^2\right)} - \alpha\sqrt{-q}cosh\left\{2\sqrt{-q}(\theta+\delta)\right\}}\right]^2 \tag{71}$$

$$\xi_{28}(x,t) = \frac{8\left(\sqrt{h}\right)^6 q\gamma^2}{9\epsilon} - \frac{4\left(\sqrt{h}\right)^6 \gamma^2}{3\epsilon}\left[\frac{-\sqrt{-q\left(\alpha^2+\beta^2\right)} - \alpha\sqrt{-q}cosh\left\{2\sqrt{-q}(\theta+\delta)\right\}}{\alpha sinh\left\{2\sqrt{-q}(\theta+\delta)\right\}+\beta}\right]^2 - \frac{4\left(\sqrt{h}\right)^6 q^2\gamma^2}{3\epsilon}\left[\frac{\alpha sinh\left\{2\sqrt{-q}(\theta+\delta)\right\}+\beta}{-\sqrt{-q\left(\alpha^2+\beta^2\right)} - \alpha\sqrt{-q}cosh\left\{2\sqrt{-q}(\theta+\delta)\right\}}\right]^2 \tag{72}$$

$$\xi_{29}(x,t) = \frac{8\left(\sqrt{h}\right)^6 q\gamma^2}{9\epsilon} - \frac{4\left(\sqrt{h}\right)^6 \gamma^2}{3\epsilon}\left[\frac{-2\alpha\sqrt{-q}}{\alpha+cosh\left\{2\sqrt{-q}(\theta+\delta)\right\}-sinh\left\{2\sqrt{-q}(\theta+\delta)\right\}} + \sqrt{-q}\right]^2 - \frac{4\left(\sqrt{h}\right)^6 q^2\gamma^2}{3\epsilon}\left[\frac{\alpha+cosh\left\{2\sqrt{-q}(\theta+\delta)\right\}-sinh\left\{2\sqrt{-q}(\theta+\delta)\right\}}{-\alpha+cosh\left\{2\sqrt{-q}(\theta+\delta)\right\}-sinh\left\{2\sqrt{-q}(\theta+\delta)\right\}}\right]^2 \tag{73}$$

$$\xi_{30}(x,t) = \frac{8\left(\sqrt{h}\right)^6 q\gamma^2}{9\epsilon} - \frac{4\left(\sqrt{h}\right)^6 \gamma^2}{3\epsilon}\left[\frac{2\alpha\sqrt{-q}}{\alpha+cosh\left\{2\sqrt{-q}(\theta+\delta)\right\}+sinh\left\{2\sqrt{-q}(\theta+\delta)\right\}} - \sqrt{-q}\right]^2 - \frac{4\left(\sqrt{h}\right)^6 q^2\gamma^2}{3\epsilon}\left[\frac{\alpha+cosh\left\{2\sqrt{-q}(\theta+\delta)\right\}+sinh\left\{2\sqrt{-q}(\theta+\delta)\right\}}{\alpha-cosh\left\{2\sqrt{-q}(\theta+\delta)\right\}-sinh\left\{2\sqrt{-q}(\theta+\delta)\right\}}\right]^2 \tag{74}$$

Case II: When $q > 0$:

$$\xi_{31}(x,t) = \frac{8\left(\sqrt{h}\right)^6 q\gamma^2}{9\epsilon} - \frac{4\left(\sqrt{h}\right)^6 \gamma^2}{3\epsilon}\left[\frac{\sqrt{q\left(\alpha^2-\beta^2\right)} - \alpha\sqrt{q}cos\left\{2\sqrt{q}(\theta+\delta)\right\}}{\alpha sin\left\{2\sqrt{q}(\theta+\delta)\right\}+\beta}\right]^2 - \frac{4\left(\sqrt{h}\right)^6 q^2\gamma^2}{3\epsilon}\left[\frac{\alpha sin\left\{2\sqrt{q}(\theta+\delta)\right\}+\beta}{\sqrt{q\left(\alpha^2-\beta^2\right)} - \alpha\sqrt{q}cos\left\{2\sqrt{q}(\theta+\delta)\right\}}\right]^2 \tag{75}$$

$$\xi_{32}(x,t) = \frac{8\left(\sqrt{h}\right)^6 q\gamma^2}{9\epsilon} - \frac{4\left(\sqrt{h}\right)^6 \gamma^2}{3\epsilon}\left[\frac{-\sqrt{q\left(\alpha^2-\beta^2\right)} - \alpha\sqrt{q}cos\left\{2\sqrt{q}(\theta+\delta)\right\}}{\alpha sin\left\{2\sqrt{q}(\theta+\delta)\right\}+\beta}\right]^2 - \frac{4\left(\sqrt{h}\right)^6 q^2\gamma^2}{3\epsilon}\left[\frac{\alpha sin\left\{2\sqrt{q}(\theta+\delta)\right\}+\beta}{-\sqrt{q\left(\alpha^2-\beta^2\right)} - \alpha\sqrt{q}cos\left\{2\sqrt{q}(\theta+\delta)\right\}}\right]^2 \tag{76}$$

$$\xi_{33}(x,t) = \frac{8\left(\sqrt{h}\right)^6 q\gamma^2}{9\epsilon} - \frac{4\left(\sqrt{h}\right)^6 \gamma^2}{3\epsilon}\left[\frac{-2i\alpha\sqrt{q}}{\alpha + cos\{2\sqrt{q}(\theta+\delta)\} - isin\{2\sqrt{q}(\theta+\delta)\}} + i\sqrt{q}\right]^2 + \frac{4\left(\sqrt{h}\right)^6 q^2\gamma^2}{3\epsilon}\left[\frac{\alpha + cos\{2\sqrt{q}(\theta+\delta)\} - isin\{2\sqrt{q}(\theta+\delta)\}}{-\alpha + cos\{2\sqrt{q}(\theta+\delta)\} - isin\{2\sqrt{q}(\theta+\delta)\}}\right]^2 \tag{77}$$

$$\xi_{34}(x,t) = \frac{8\left(\sqrt{h}\right)^6 q\gamma^2}{9\epsilon} - \frac{4\left(\sqrt{h}\right)^6 \gamma^2}{3\epsilon}\left[\frac{2i\alpha\sqrt{q}}{\alpha + cos\{2\sqrt{q}(\theta+\delta)\} + isin\{2\sqrt{q}(\theta+\delta)\}} - i\sqrt{q}\right]^2 + \frac{4\left(\sqrt{h}\right)^6 q^2\gamma^2}{3\epsilon}\left[\frac{\alpha + cos\{2\sqrt{q}(\theta+\delta)\} + isin\{2\sqrt{q}(\theta+\delta)\}}{\alpha - cos\{2\sqrt{q}(\theta+\delta)\} - isin\{2\sqrt{q}(\theta+\delta)\}}\right]^2 \tag{78}$$

Case III: When $q = 0$:

$$\xi_{35}(x,t) = -\frac{4\left(\sqrt{h}\right)^6 \gamma^2}{3\epsilon}\frac{1}{(\theta+\delta)^2} \tag{79}$$

This equation is exactly the same as Eq. (50).

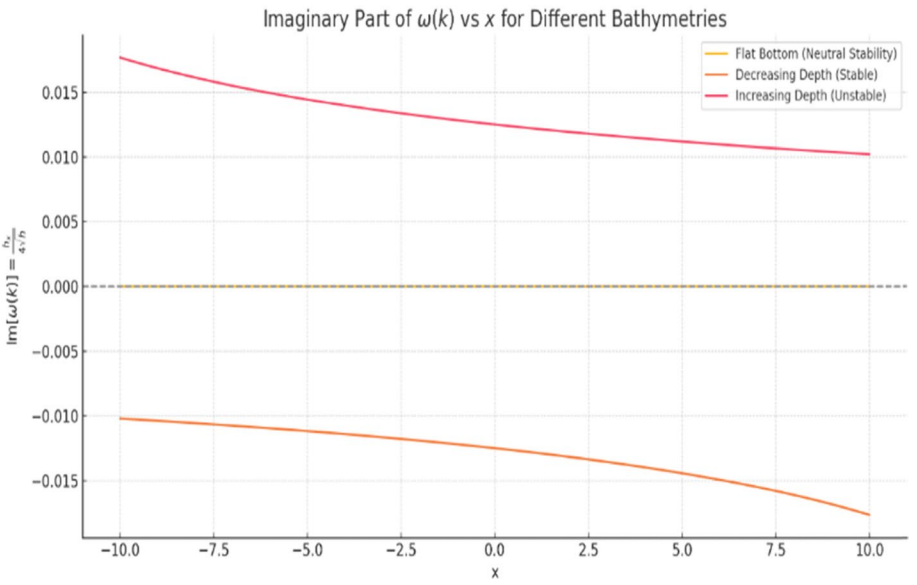

Fig. 1 Stability analysis of Eq. (1)

4 Analysis

4.1 Wave Number Calculation

To analyze the exact solution and perform spectral analysis of ocean waves, it's essential to calculate the wave number using the following dispersion relation [22, 49]:

$$\omega^2 = gktanh\,(kh) \tag{80}$$

where ω is the angular frequency, g is the gravitational acceleration, k is the wave number, and h is the water depth. The angular frequency is determined by $\omega = \frac{2\pi}{T}$, with T as the wave period. Since this equation is transcendental, it requires numerical solutions, often using iterative methods like the Newton-Raphson technique, to accurately figure out k. Initial estimates can be adjusted based on deep or shallow water conditions. After calculating the wave number, we can effectively characterize the exact solution and related analysis.

4.2 Stability Analysis

We conduct a thorough linear stability study of the solutions we have produced. Our fundamental objective is to comprehend the behavior of these solutions and their integrity when faced with diverse bathymetries, including changing undersea depths and topographical characteristics. This investigation is essential for evaluating the dependability and adaptability of our solutions in real-world scenarios when the seabed profile is heterogeneous. By assessing stability across these varied situations, we can ascertain the scope of applicability and possible constraints of our findings.

To do a linear stability analysis of the specified exact solution of $\xi_{35}(x,t)$, Consider a small fluctuation $\psi\,(x,\,t)$ in relation to the precise solution $\xi_{23}(x,t)$, thus [1, 36, 45]:

$$\xi(x,t) = €\xi(x,t) + \xi_{23}(x,t); \quad 0 < € \ll 1. \tag{81}$$

In the Eq. (1), substitute, and make sure that only linear terms are kept in which yields:

$$\xi_t + \sqrt{h}\xi_x + \frac{h_x}{4\sqrt{h}}\xi + \frac{3\varepsilon}{2\sqrt{h}}(\xi_{23}\xi_x + \xi\xi_{23,x}) + \frac{\gamma^2 h^{\frac{5}{2}}}{6}\xi_{xxx} = 0 \tag{82}$$

Let's assume that the perturbation has a solution in the normal mode as follows:

$$\xi(x,t) = e^{i(kx-\omega t)} \tag{83}$$

The result of differentiating it with regard to time and space and substituting the equation discussed before is as follows:

$$-i\omega + ik\sqrt{h} + \frac{h_x}{4\sqrt{h}} + \frac{3\varepsilon}{2\sqrt{h}}\left(ik\xi_{23} + \xi_{23,x}\right) - i\frac{\gamma^2 h^{\frac{5}{2}}}{6}k^3 = 0 \tag{84}$$

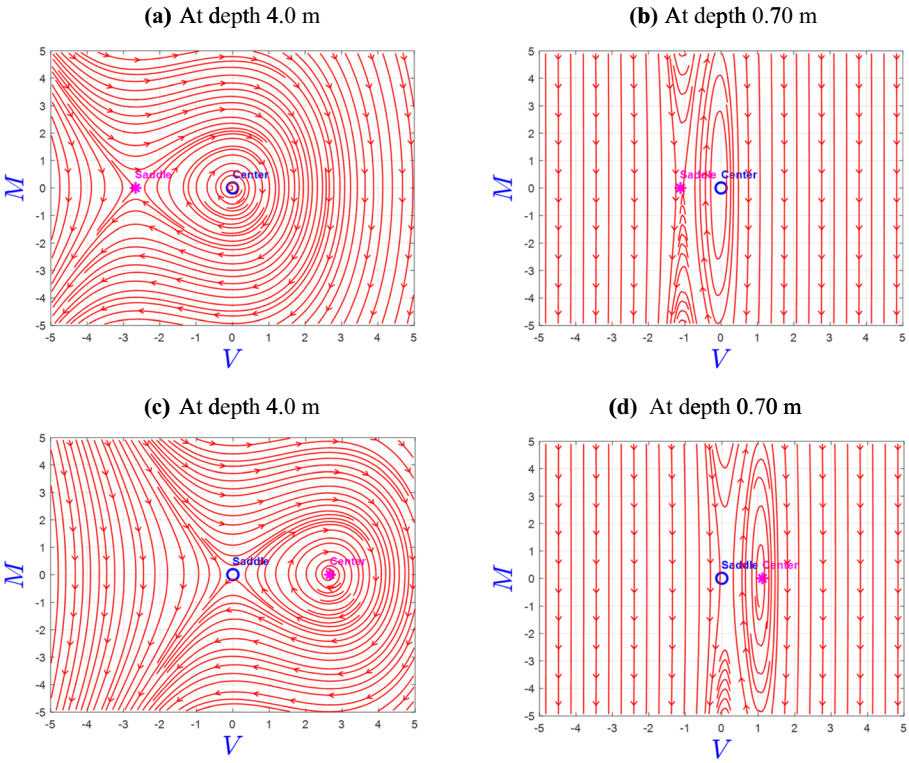

Fig. 2 The phase diagram of Eq. (1), where $\gamma = 0.1, \varepsilon = 0.1$

The dispersion relation can be obtained by disregarding the values of $\xi_{23,x}$ at the level of tiny spatial variation which is:

$$\omega(k) = i\sqrt{h} + i\frac{h_x}{4\sqrt{h}} + \frac{3\varepsilon}{2\sqrt{h}}k\xi_{23} - \frac{\gamma^2 h^{\frac{5}{2}}}{6}k^3 = 0 \tag{85}$$

Therefore the stability criterion is set as follows:

If $Im(\omega(k)) = 0$ then ξ oscillates, i.e. stable; $Im(\omega(k)) > 0$ then ξ grows exponentially, i.e. unstable and $Im(\omega(k)) < 0$ then ξ decays, i.e. stable, where $Im(\omega(k)) = \frac{h_x}{4\sqrt{h}}$. So, the stability depends on h_x.

If $h_x > 0$ (increasing depth), the solution is unstable; $h_x < 0$ (decreasing depth), the solution is stable and $h_x = 0$ (flatbed), the solution is neutrally stable (Fig. 1).

For various bottom topographies, the plot illustrates the imaginary component of the wave frequency (k), which is responsible for determining the stability of wave solutions when subjected to tiny perturbations. The fact that this is the case demonstrates that the variation of the water depth $h(x)$ has a considerable impact on the stability of this particular solution. This scenario holds true for all the derived solutions, highlighting the profound impact of bottom topography on wave stability.

4.3 Bifurcation

This analysis aims to thoroughly examine the system by calculating the Jacobian matrix, determining the eigenvalues, and identifying the equilibrium points. By conducting this analysis, we can discern the nature of the equilibrium points, categorizing them as saddle points, center points, or cuspidal points. Additionally, this approach will enable us to comprehend the phase portrait of the equation more effectively. Suppose the planar dynamical system is characterized by the following equations, resulting from a Galilean transformation applied to the original ODEs [50–52]:

$$\left.\begin{aligned} V' &= M \\ M' &= -\kappa V^2 - \chi V \end{aligned}\right\} \tag{86}$$

where V and M stands for the state parameters, and $\kappa = \frac{9\epsilon}{4h^3\gamma^2}$, and $\chi = \frac{6\varpi}{h^{5/2}\gamma^2}$ are arbitrary constants.

The resulting Hamiltonian function is as follows:

$$H(V,M) = \frac{1}{2}M^2 + \left(\frac{\chi}{2}V^2 + \frac{\kappa}{3}V^3\right) = h \tag{87}$$

The term $\frac{1}{2}M^2$ of Eq. (86) represent the kinetic energy, the term $\left(\frac{\chi}{2}V^2 + \frac{\kappa}{3}V^3\right)$ of Eq. (86) is the potential energy of the system, and h represents the Hamiltonian constant.

The equilibrium points are found by setting the system to zero. Solving this system provides the equilibrium points $\left(e_1, e_2\right)$ as follows:

$$\left.\begin{aligned} e_1 &= (0,0) \\ e_2 &= \left(\tfrac{-\chi}{\kappa}, 0\right) \end{aligned}\right\} \tag{88}$$

Now, the Jacobian matrix of the given system is as follows:

$$J(V,M) = \begin{vmatrix} 0 & 1 \\ -2\kappa V - \chi & 0 \end{vmatrix} \tag{89}$$

The characteristic equation, $|J(V,M) - \lambda I|$ that bears the eigenvalues $\left(\lambda_1, \lambda_2\right)$ at the equilibrium points $\left(e_1, e_2\right)$ as follows:

$$\left.\begin{aligned} \lambda_{e_1} &= \pm i\sqrt{\chi} \\ \lambda_{e_2} &= \pm\sqrt{\chi} \end{aligned}\right\} \tag{90}$$

So, the equilibrium points are categorized into the following cases:

Case I: If $\varpi(0.1) > 0$, at e_1 the eigenvalues are purely imaginary $\left(\pm i\sqrt{\chi}\right)$, indicating a center point. Also, at e_2 the eigenvalues are real and distinct $\left(\pm\sqrt{\chi}\right)$, showing a saddle point (Fig. 2(a) and (b)). The corresponding values of the parameters are given in the caption of the figure.

Case II: If $\varpi(-0.1) < 0$, at e_1 the eigenvalues are real and distinct $\left(\pm\sqrt{\chi}\right)$, showing a saddle point. Similarly, at e_2 the eigenvalues are purely imaginary $\left(\pm i\sqrt{\chi}\right)$, writing down a center point (Fig. 2(c) and (d)). The corresponding values of the parameters are given in the caption of the figure.

No cuspidal points are found in this analysis based on the given system. It is observed that, depending on the properties of the nonlinear variables, the Hartman-Grobman theorem indicates that a linearised system displaying a centre may coincide with either a centre or a focus in the whole nonlinear system. The current analysis demonstrates that the phase portraits (refer to Fig. 2 (a, b, c, d)) distinctly show closed orbits surrounding the equilibrium point, with no evidence of spiralling behaviour. This statement verifies that the equilibrium acts as a centre within the nonlinear system, suggesting that the nonlinear terms do not contribute to damping or instability near the equilibrium point.

5 Visual Representation of the Exact Solutions

To visualize and analyze the exact solutions, we used Mathematica, a computational tool well-known for its advanced mathematical computation and visualization capabilities. We utilized various types of visualizations, including 3D plots, 2D plots, and density plots, to provide a comprehensive view of the solutions' behaviors and characteristics. For each method, we examined the solutions within the domain $-20 \leq (x, t) \leq 20$, and included parameter values in the figure descriptions to facilitate precise replication and verification.

In our 2D plots, we combined multiple graphs into a single figure by varying the parameter t, allowing us to compare how the solutions evolve over time. This approach provides insights into the temporal dynamics and stability of the solutions. By integrating these visual perspectives, we offer a detailed understanding of the mSKdV equation's solutions.

5.1 Visualization Through $\left(\frac{G'}{G}, \frac{1}{G}\right)$- Expansion Method

Figures 3, 4 and 5.

5.2 Visualization via Unified Method

Figures 6, 7 and 8.

5.3 Discussion of the Figures

This section of the study provides a detailed presentation of various soliton solutions obtained using two different methods: the $\left(\frac{G'}{G}, \frac{1}{G}\right)$ technique, and the unified method. Figures 3, 4 and 5 showcase soliton behaviors generated by the $\left(\frac{G'}{G}, \frac{1}{G}\right)$ technique, demonstrating the impact of different parameters at water depths of 4 meters and 0.7 meters.

In Fig. 3, a periodic soliton is presented, exhibiting a stable and repeating wave profile that can be related to the behavior of long ocean waves, such as tsunamis, as they propagate and interact with the continental shelf. Figure 4 depicts a bright soliton with a distinct localized peak, evolving into a single soliton at a depth of 0.7 meters—an effect analogous to amplitude focusing observed in coastal engineering, where wave transformation is

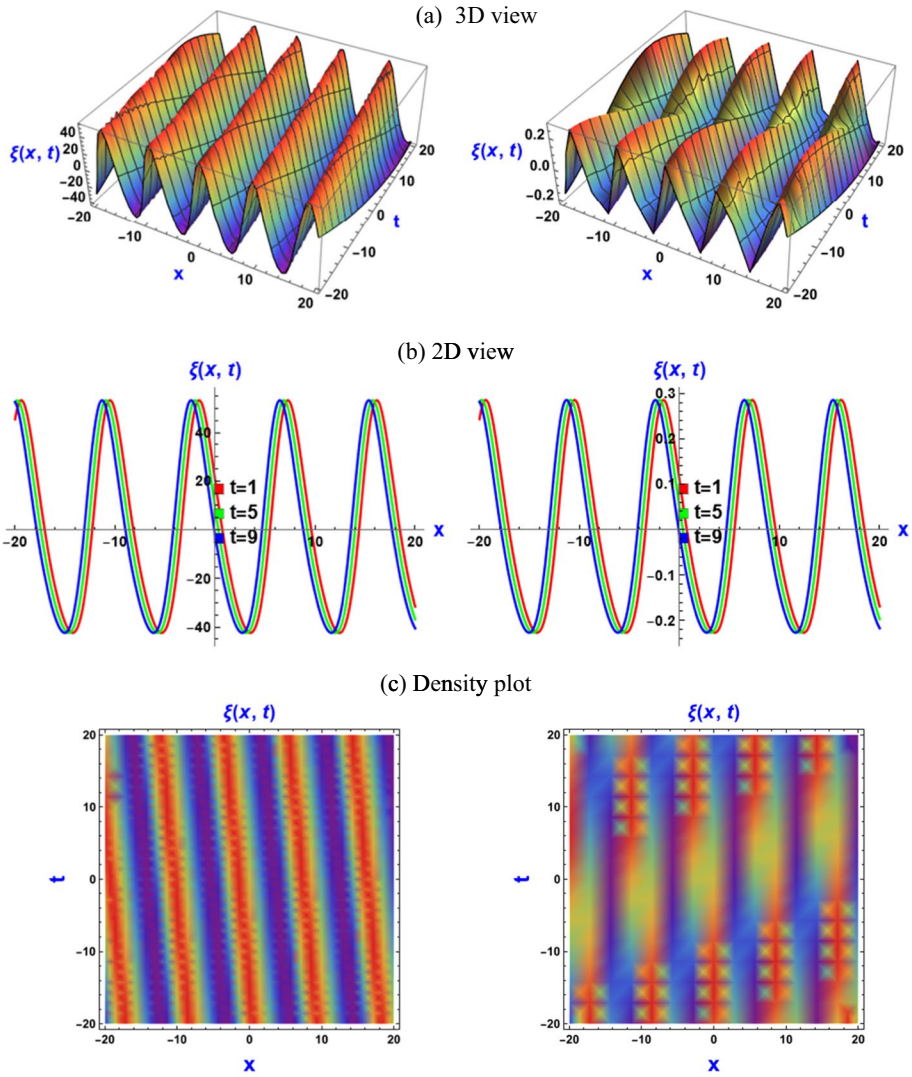

Fig. 3 Variation of the wave profile of the exact solution of Eq. (26) showing periodic solitons across different plots, where $m_1 = 1.00, m_2 = 0.10, \eta = 3.0, \epsilon = 0.25, \wp = 0.5$, and $\gamma = 1.5$. (**a**) 3D view. (**b**) 2D view. (**c**) Density plot

strongly influenced by bathymetric variations. Furthermore, Fig. 5 illustrates dark soliton structures at depths of 4 meters and 0.7 meters, reflecting features similar to internal waves in stratified oceans with slowly varying density profiles. These examples highlight the broader physical significance of soliton dynamics in geophysical and engineering contexts, particularly in predicting and managing wave behavior in natural and built environments. The soliton characteristics are mainly determined by parameters such as k, $\wp$, m, and the incident wave parameters. The specific values of these parameters dictate the type and form of the solitons observed.

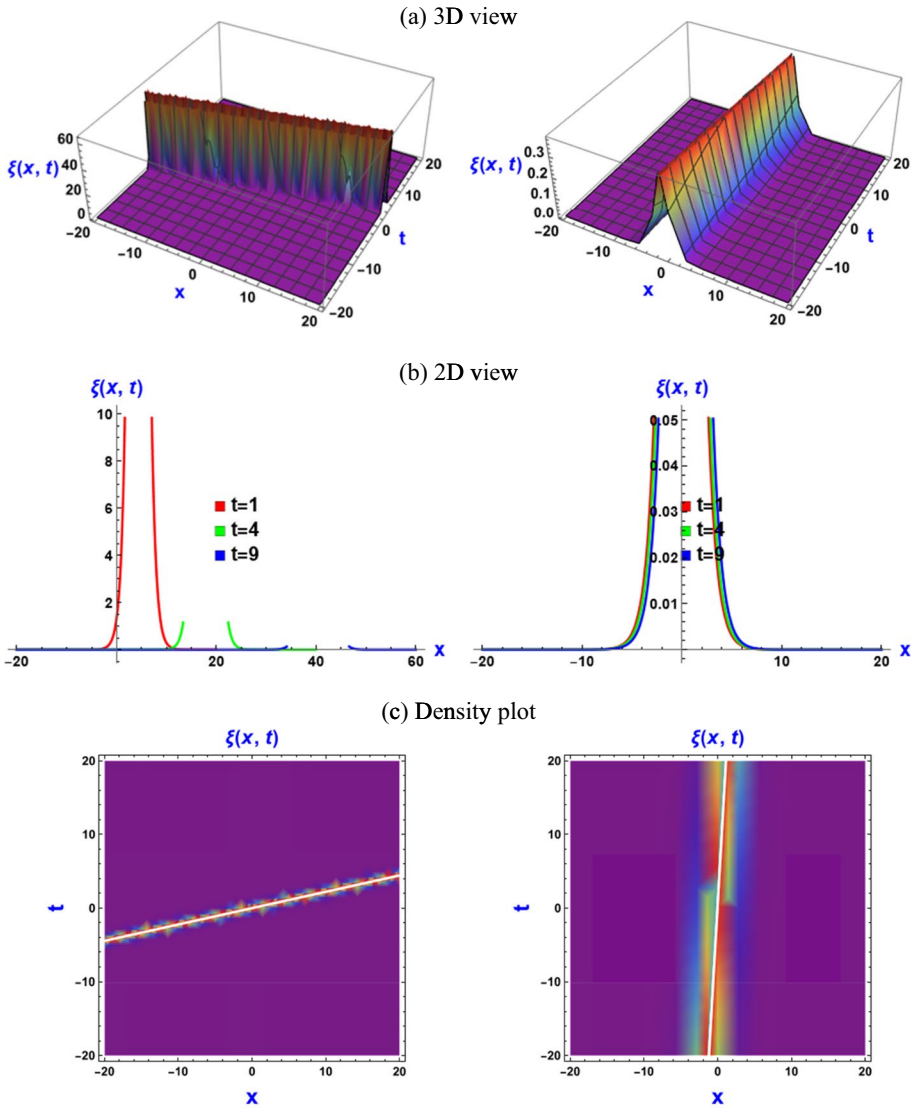

Fig. 4 Variation of the bright soliton of Eq. (34) throughout various scenarios, where $m_1 = 1.00, m_2 = 0.10, \eta = 0.10, \epsilon = 0.25, \wp = -1.50$, and $\gamma = 0.75$. (**a**) 3D view. (**b**) 2D view. (**c**) Density plot

Figures 6, 7 and 8 examine soliton structures using the unified method. Figure 6 illustrates the transition from a multi-soliton state to a breather soliton, highlighting the dynamic modulation of amplitude and waveform. Such behavior can be linked to the evolution of tsunami wave trains, where nonlinear interactions and varying bathymetry may cause initially separated wave packets to merge into more complex structures. Figure 7 presents a quasi-breather soliton, a localized solution that exhibits enhanced oscillatory modes due to its underlying spectral complexity. This type of behavior is

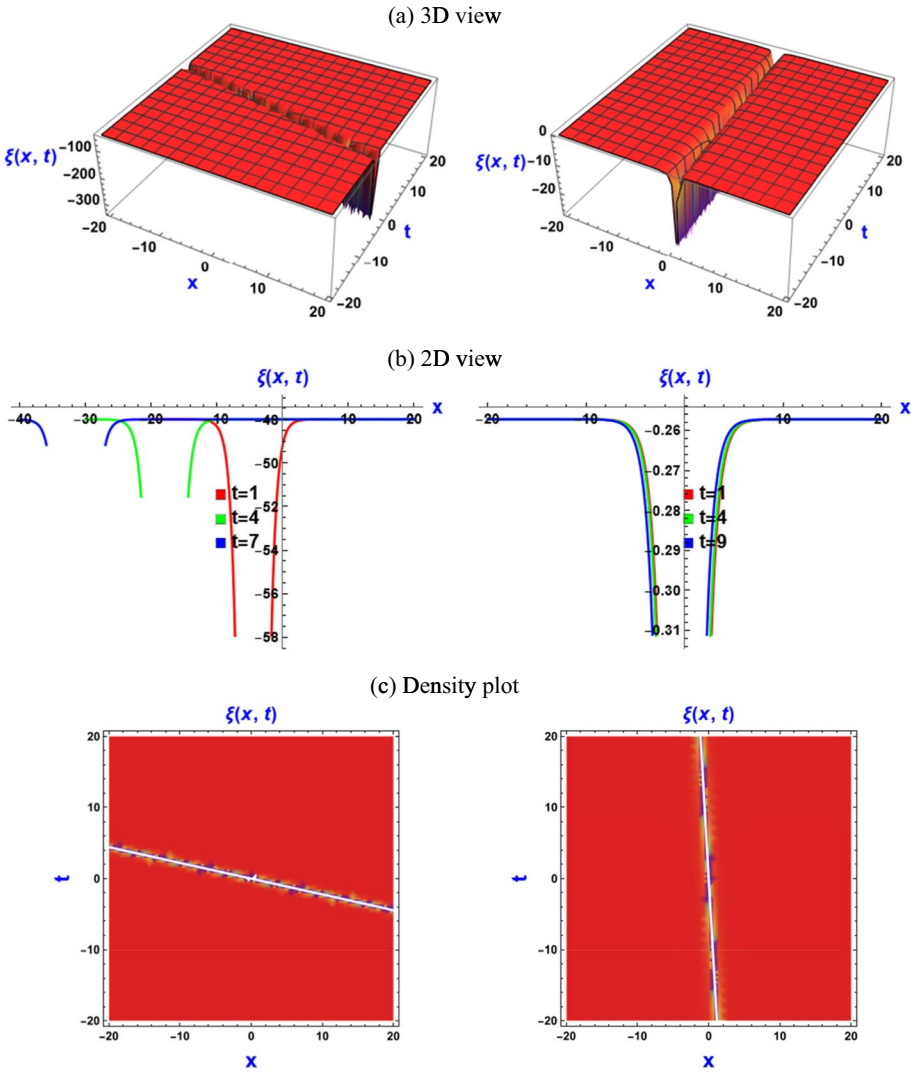

Fig. 5 Variation of the dark soliton of Eq. (38) within distinct plots, where $m_1 = 1.00, m_2 = 0.10, \eta = 0.01$, $\epsilon = 0.25$, $\wp = -1.50$, and $\gamma = 0.75$. (**a**) 3D view. (**b**) 2D view. (**c**) Density plot

analogous to internal wave dynamics in stratified oceans, where energy transfer among different modes leads to rich oscillatory patterns that play a key role in mixing processes and energy distribution. Figure 8 depicts breather solitons, characterized by temporally confined oscillations that repeat periodically. This phenomenon reflects important processes in coastal engineering, where the periodic focusing and defocusing of wave energy can significantly influence nearshore wave transformation, coastal structure stability, and shoreline evolution. Together, these figures demonstrate how breather-type soliton dynamics not only enrich the mathematical theory of nonlinear wave propagation

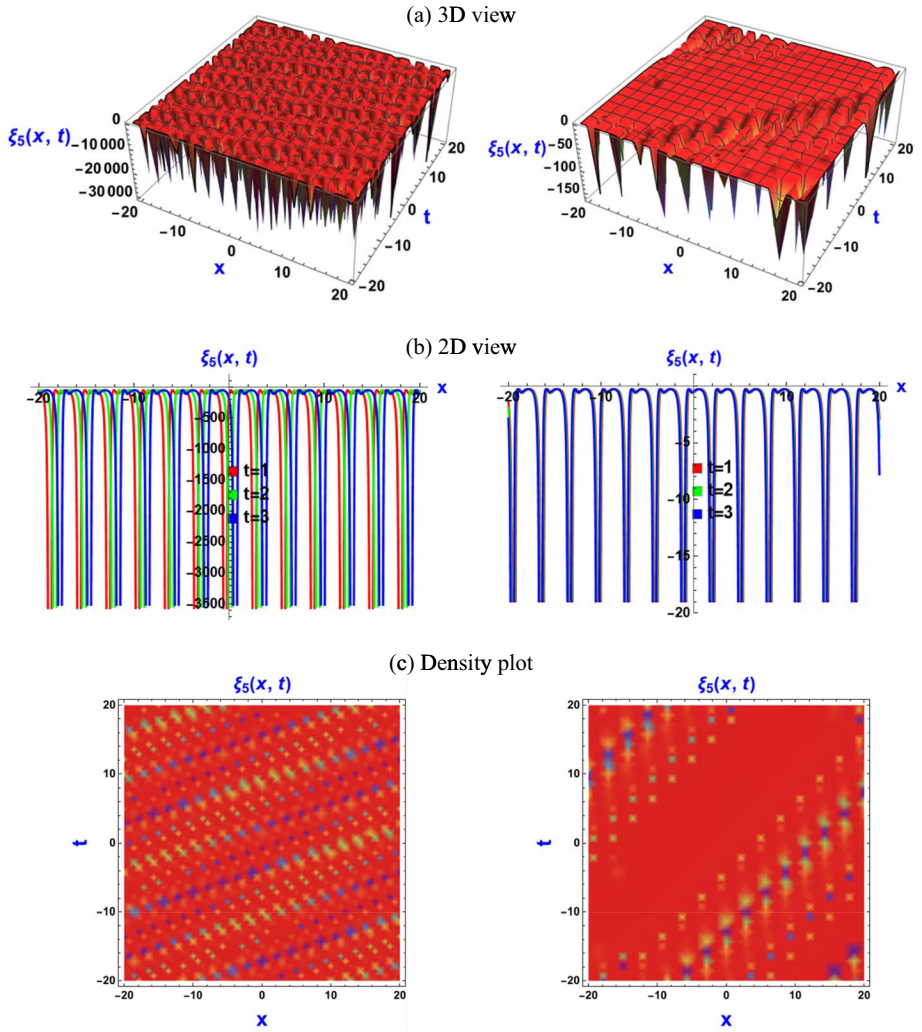

Fig. 6 Variations of periodic multi soliton to breather solitons across different plots, where = 5.10, $\beta = 5.30$, $q = 1.05$, $\delta = 0.15$, $\epsilon = 0.50$, and $\gamma = 0.25$. (**a**) 3D view. (**b**) 2D view.(**c**) Density plot

but also provide insights into practical geophysical and engineering problems, from tsunami evolution to internal oceanic waves and coastal wave-structure interactions.

Within this framework, parameters such as k, q and the incident wave parameters play significant roles in shaping soliton behavior. Particularly, the parameter k, and incident wave parameters have a strong influence.

This study highlights the role of different mathematical methods and parameter variations in understanding and visualizing soliton dynamics, especially within the context of the mSKdV equation. By examining the interaction of these factors, the research provides valuable insights into the complex behavior of solitons under various conditions and mathematical frameworks.

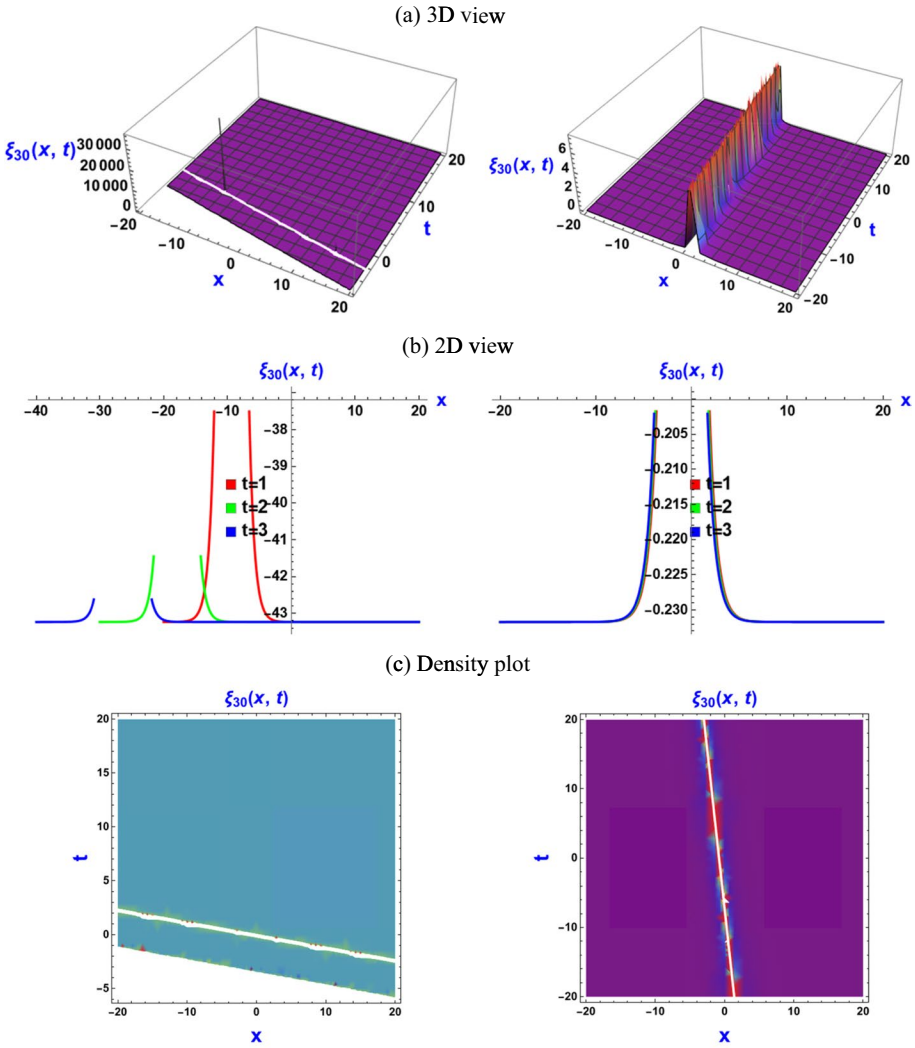

Fig. 7 Variations of quasi-breather soliton across several plots, where $= 0.50, q = -0.40$, $\delta = 0.25$, $\epsilon = 0.25$, and $\gamma = 0.50$. (**a**) 3D view. (**b**) 2D view. (**c**) Density plot

6 Conclusion

This research provides a groundbreaking analysis of wave transformations in shallow water areas using the one-dimensional mSKdV equation for the first time. By utilizing the $\left(\frac{G'}{G}, \frac{1}{G}\right)$ method alongside the unified method, the study successfully derives solitary wave solutions that illuminate the complex dynamics of waves as they approach the shore. The importance of predicting wave climates in these regions is underscored, particularly due to the significant effects of wave transformations on sediment transport, circulation, and other nearshore processes. Through bifurcation analysis, the phase portrait of the mSKdV equation is detailed, revealing a wide range of soliton behaviors.

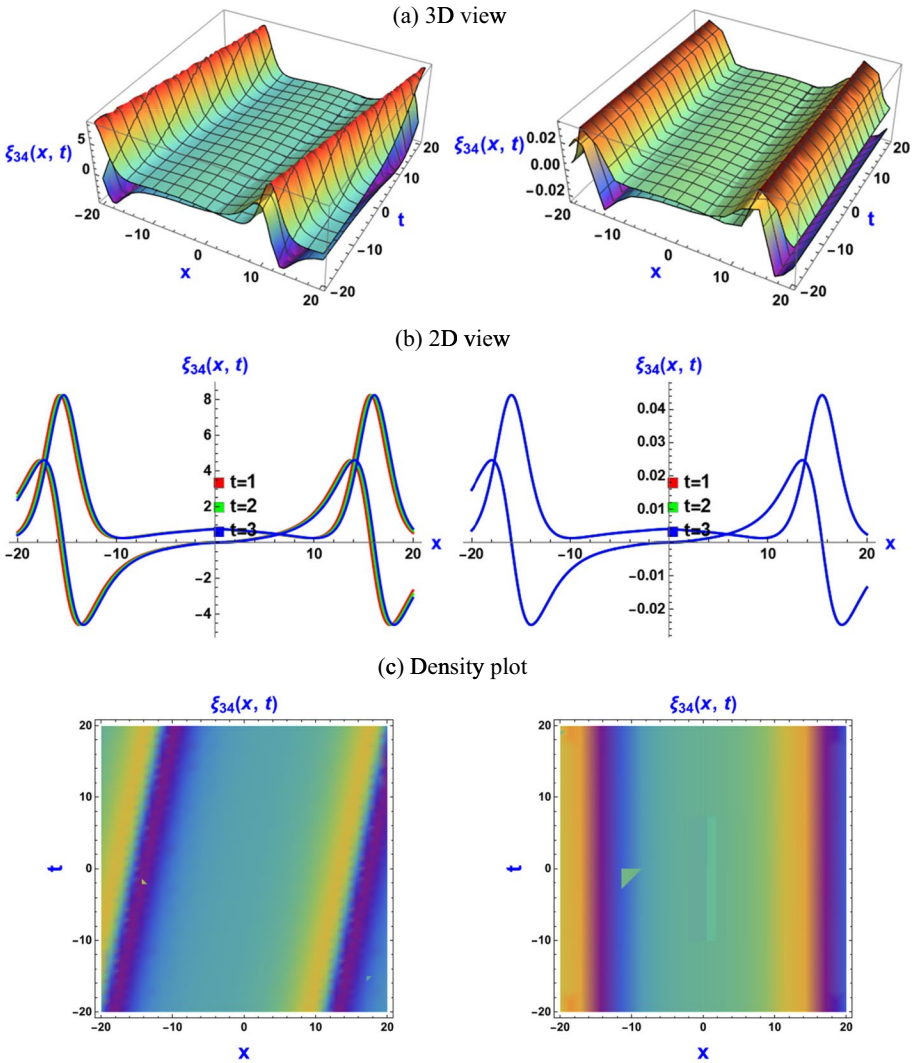

Fig. 8 Variations of breather soliton across different plots, where $= 0.50, q = 0.01, \delta = 0.25, \epsilon = 0.25$, and $\gamma = 0.50$. (**a**) 3D view. (**b**) 2D view. (**c**) Density plot

Also linear stability analysis clearly showed the significant influence of varying bathymetries on the stability of wave solutions. The imaginary component of the wave frequency consistently demonstrated that water depth significantly influences solution stability across all derived cases. The findings highlighted the critical importance of bottom topography in the prediction and comprehension of wave behavior. The exact solutions are represented through 3D plots, 2D plots with temporal changes, and density plots, capturing the various soliton dynamics within shallow water environments. These include periodic solitons, bright and dark solitons, periodic breathers, breather,

quasi-breathers, and single solitons, each offering unique insights into wave behavior as they move from deeper waters toward the shoreline. The findings of this study make a significant contribution to coastal engineering by deepening our understanding of soliton solutions for the mSKdV equation. Predicting and modeling these wave transformations are essential for developing effective coastal management strategies, particularly in reducing the impacts of erosion and sediment displacement. Furthermore, the methodologies developed in this research provide a solid foundation for future studies focused on exploring nonlinear wave phenomena in various coastal contexts. Overall, this work not only advances theoretical understanding but also has practical implications for the sustainable management of coastal regions amid the challenges posed by dynamic oceanic processes.

Acknowledgements The authors would like to acknowledge the Deanship of Graduate Studies and Scientific Research, Taif University for funding this work.

Author Contributions M.N.H., I.A., A.M.S. and K.E-R. wrote the main manuscript text, and M.N.H., M.M.M. and W-X. M. prepared all the figures and supervised this research. All authors reviewed the manuscript.

Funding Not applicable.

Data Availability All data generated or analyzed during this study are included in this article.

Declarations

Competing interests The authors declare no competing interests.

Ethical Approval I hereby declare that this manuscript is the result of my independent creation under the reviewers' comments. Except for the quoted contents, this manuscript does not contain any research achievements that have been published or written by other individuals or groups.

References

1. Hossain, M.N., Miah, M.M., Duraihem, F.Z., Rehman, S.: Stability, modulation instability, and analytical study of the confirmable time fractional Westervelt equation and the Wazwaz Kaur Boussinesq equation. Optical and Quantum Electronics **56**, 1–29 (2024). https://doi.org/10.1007/s11082-024-06776-y
2. Younas, U., Younis, M., Seadawy, A.R., Rizvi, S.T.R., Althobaiti, S., Sayed, S.: Diverse exact solutions for modified nonlinear Schrödinger equation with conformable fractional derivative. Results in Physics **20**, 103766 (2021). https://doi.org/10.1016/j.rinp.2020.103766
3. Islam, S.M.R., Wang, H.: Some Analytical Soliton Solutions of the Nonlinear Evolution Equations. *J. Ocean Eng. Sci.* 1–9 (2022), https://doi.org/10.1016/j.joes.2022.05.013.
4. Ismael, H.F., Bulut, H.: Nonlinear Dynamics of (2+1)-Dimensional Bogoyavlenskii-Schieff Equation Arising in Plasma Physics. Math. Methods Appl. Sci. **44**(13), 10321–10330 (2021). https://doi.org/10.1002/mma.7372
5. Rafiq, M.N., Rafiq, M.H., Alsaud, H.: Chaotic response, multistability and new wave structures for the generalized coupled Whitham–Broer–Kaup–Boussinesq–Kupershmidt system with a novel methodology. Chaos, Solitons & Fractals **190**, 115755 (2025). https://doi.org/10.1016/j.chaos.2024.115755
6. Hossain, M.D., Boulaaras, S.M., Saeed, A.M., Gissy, H., Hossain, M.N., Miah, M.M.: New investigation on soliton solutions of two nonlinear PDEs in mathematical physics with a dynamical property: bifurcation analysis. Open Physics **23**(1), 20250155 (2025). https://doi.org/10.1515/phys-2025-0155

7. Rafiq, M.N., Rafiq, M.H., Alsaud, H.: New Insights into the Diversity of Stochastic Solutions and Dynamical Analysis for the Complex Cubic NLSE with δ-Potential through Brownian Process. Communications in Theoretical Physics (2025). https://doi.org/10.1088/1572-9494/adaddd
8. Ismael, H.F., Sulaiman, T.A., Osman, M.S.: Multi-Solutions with Specific Geometrical Wave Structures to a Nonlinear Evolution Equation in the Presence of the Linear Superposition Principle. Commun. Theor. Phys. **75**(1), 015001 (2022). https://doi.org/10.1088/1572-9494/ac42ba
9. Iqbal, M., Seadawy, A.R., Lu, D., Zhang, Z.: Computational approach and dynamical analysis of multiple solitary wave solutions for nonlinear coupled Drinfeld–Sokolov–Wilson equation. Results in Physics **54**, 107099 (2023). https://doi.org/10.1016/j.rinp.2023.107099
10. Jafari, H., Kadkhoda, N., Baleanu, D.: Fractional lie group method of the time-fractional Boussinesq equation. Nonlinear Dyn. **81**, 1569–1574 (2015). https://doi.org/10.1007/s11071-015-2091-4
11. Bilal, M., Shafqat-Ur-Rehman, Ahmad, J.: Investigation of Optical Solitons and Modulation Instability Analysis to the Kundu–Mukherjee–Naskar Model. Opt. Quantum Electron. **53**, 1–22 (2021). https://doi.org/10.1007/s11082-021-02939-3
12. Liu, J.G., Osman, M.S., Zhu, W.H., Zhou, L., Ai, G.P.: different complex wave structures described by the hirota equation with variable coefficients in inhomogeneous optical fibers. Applied Physics B **125**, 1–9 (2019). https://doi.org/10.1007/s00340-019-7287-8
13. Hossain, M.N., Alsharif, F., Miah, M.M., Kanan, M.: Abundant new optical soliton solutions to the Biswas – Milovic equation with sensitivity analysis for optimization. Mathematics **12**, 1585 (2024). https://doi.org/10.3390/math12101585
14. Rafiq, M.N., Rafiq, M.H., Alsaud, H.: Diversity of Soliton Dynamics, Positive Multi-Complexiton Solutions and Modulation Instability for (3+1)-Dimensional Extended Kairat-X Equation. Modern Phys Lett B **39**(25), 2550112 (2025)
15. Ismael, H.F., Seadawy, A., Bulut, H.: Multiple soliton, fusion, breather, lump, mixed kink-lump and periodic solutions to the extended shallow water wave model in (2+1)-dimensions. Modern Phys Lett B **35**(08), 2150138 (2021). https://doi.org/10.1142/S0217984921501385
16. Hoque, A., Rahman, M., Rahman, M., Hossain, N., Paul, G.C.: Theoretical study of spilling wave attenuation by air bubbles, turbulence, and bottom friction. Estuar. Coast. Shelf Sci. **262**, 107606 (2021). https://doi.org/10.1016/j.ecss.2021.107606
17. Hossain, M.N., Araki, S.: Transformation of significant wave height and set-up due to entrained air bubbles effect in breaking waves. Ocean Model **190**, 102403 (2024). https://doi.org/10.1016/j.ocemod.2023.102403
18. Hoque, A., Hossain, N., Ali, S., Rahman, M.: Wave breaking and bubble formation associate energy dissipation and wave setup. Ocean Dyn **69**, 913–923 (2019). https://doi.org/10.1007/s10236-019-01279-4
19. Hossain, M.N., Araki, S., Hoque, A., Josiah, N.R.: wave height distribution for plunging breakers induced by air bubbles. Ocean Eng **309**, 118472 (2024). https://doi.org/10.1016/j.oceaneng.2023.118472
20. Tran, K.Q.; Duong, N.T., Tran, L.H., Luu, L.X.: Irregular wave height transformation prediction based on weighted rayleigh distribution and bore concept. Coast. Eng. J. 1–17. (2024). https://doi.org/10.1080/21664250.2023.2166725.
21. Hossain, M.N., Araki, S.: Energy dissipation model for irregular breaking waves owing to air bubbles. Ocean Eng **266**, 112985 (2022). https://doi.org/10.1016/j.oceaneng.2022.112985
22. Türker, U., Boulanoire, S.: Wave energy converter efficiency based on wave transmission and relative capture width performance. Proc. Instit. Mech. Eng. Part M: Journal of Engineering for the Maritime Environment **238**(4), 933–942 (2024). https://doi.org/10.1177/14750902231126782
23. Hossain, M.N., Rahman, M., Hoque, A.: Statistical distribution of wave heights attenuation by entrained air bubbles in the surf zone. Ocean Eng **250**, 110911 (2022). https://doi.org/10.1016/j.oceaneng.2022.110911
24. Mase, H., Kitano, T.: Spectrum-based prediction model for random wave transformation over arbitrary bottom topography. Coastal Engineering Journal **42**, 111–151 (2000). https://doi.org/10.1142/S0578563400000067
25. Demiray, H.: Weakly nonlinear waves in water of variable depth: variable-coefficient Korteweg–de Vries equation. Comput. Math. Appl. **60**(6), 1747–1755 (2010). https://doi.org/10.1016/j.camwa.2010.06.037
26. Borhan, J.R.M., Ganie, A.H., Miah, M.M., Iqbal, M.A., Seadawy, A.R., Mishra, N.K.: A highly effective analytical approach to innovate the novel closed form soliton solutions of the Kadomtsev-Petviashivili equations with applications. Optical and Quantum Electronics **56**, 1–23 (2024). https://doi.org/10.1007/s11082-024-06706-y

27. Khan, M.A.U., Akram, G., Sadaf, M.: Dynamics of Novel Exact Soliton Solutions of Concatenation Model Using Efective Techniques. Opt. Quantum Electron **56**, 385 (2024). https://doi.org/10.1007/s11082-023-05957-5
28. Fan, E.: Extended tanh-function method and its applications to nonlinear equations. Phys. Lett. A **277**, 212–218 (2000). https://doi.org/10.1016/S0375-9601(00)00725-8
29. Ma, W.X., Zhu, Z.: Solving the (3 + 1)-dimensional generalized KP and BKP equations by the multiple exp-function algorithm. Applied Mathematics and Computation **218**, 11871–11879 (2012). https://doi.org/10.1016/j.amc.2012.05.049
30. Kumar, A., Pankaj, R.D.: Tanh-coth scheme for traveling wave solutions for nonlinear wave interaction model. Journal of the Egyptian Mathematical Society **23**, 282–285 (2015). https://doi.org/10.1016/j.joems.2014.05.002
31. Kawser, M.A., Ali Akbar, M., Khan, M.A., Ghazwan, H.A.: Exact soliton solutions and the signifcance of time-dependent coefcients in the boussinesq equation: theory and application in mathematical physics. Sci. Rep. **14**, 762 (2024). https://doi.org/10.1038/s41598-023-50782-1
32. Hossain, M.N., El Rashidy, K., Alsharif, F., Kanan, M., Ma, W.-X., Miah, M.M.: New optical soliton solutions to the Biswas – Milovic equations with power law and parabolic law nonlinearity using the Sardar - subequation method. Opt. Quantum. Electron. **56**, (2024). https://doi.org/10.1007/s11082-024-07073-4.
33. Ismael, H.F., Bulut, H., Baskonus, H.M., Gao, W.: Newly modified method and its application to the coupled boussinesq equation in ocean engineering with its linear stability analysis. Commun Theor. Phys. **72**(11), 115002 (2020). https://doi.org/10.1088/1572-9494/aba70e
34. Zafar, A., Raheel, M., Ali, K.K., Razzaq, W.: On optical soliton solutions of new Hamiltonian amplitude equation via Jacobi elliptic functions. Eur. Phys. J. Plus **135**, 1–17 (2020). https://doi.org/10.1140/epjp/s13360-020-00694-0
35. Babajanov, B., Abdikarimov, F.: The application of the functional variable method for solving the loaded non-linear evaluation equations. Front. Appl. Math. Stat. **8**, 1–9 (2022). https://doi.org/10.3389/fams.2022.912674
36. Hossain, M.N., Miah, M.M., Abbas, M.S., El-Rashidy, K., Borhan, J.R.M., Kanan, M.: An analytical study of the Mikhailov – Novikov – Wang equation with stability and modulation instability analysis in industrial engineering via multiple methods. Symmetry **16**, 879 (2024). https://doi.org/10.3390/sym16070879
37. Habib, M.A., Ali, H.M.S., Miah, M.M., Akbar, M.A.: The generalized Kudryashov method for new closed form traveling wave solutions to some NLEEs. AIMS Mathematics **4**, 896–909 (2019). https://doi.org/10.3934/math.2019.3.896
38. Iqbal, M.A., Miah, M.M., Rasid, M.M., Alshehri, H.M., Osman, M.S.: An investigation of two integro-differential KP hierarchy equations to find out closed form solitons in mathematical physics. Arab Journal of Basic and Applied Sciences **30**, 535–545 (2023). https://doi.org/10.1080/25765299.2023.2256049
39. Rafiq, M.H., Lin, J.: Periodic breather waves, stripe-solitons and interaction solutions for the (3+1)-dimensional variable-coefficient Kadomtsev–Petviashvili-like equation. Chaos Solitons Fractals **194**, 116212 (2025). https://doi.org/10.1016/j.chaos.2024.116212
40. Hossain, M.N., Rasid, M.M., Abouelfarag, I., El-Rashidy, K., Miah, M.M., Kanan, M.: A new investigation of the extended Sakovich equation for abundant soliton solution in industrial engineering via two efficient techniques. Open Physics **22**(1), 20240096 (2024). https://doi.org/10.1515/phys-2024-0096
41. Zayed, E.M.E., Alurrfi, K.A.E.: The (G'/G, 1/G)-expansion method and its applications for solving two higher order nonlinear evolution equations. Mathematical Problems in Engineering **2014**, 1–20 (2014)
42. Vivas-Cortez, M., Akram, G., Sadaf, M., Arshed, S., Rehan, K., Farooq, K.: Traveling wave behavior of new (2+1)-dimensional combined KdV–MKdV equation. Results Phys. **45**, 106244 (2023). https://doi.org/10.1016/j.rinp.2023.106244
43. Yue, X., Kaplan, M., Kaabar, M.K.A., Yang, H.: Exploring new features for the (2+1)-dimensional Kundu–Mukherjee–Naskar equation via the techniques of (G'/G,1/G)-expansion and exponential rational function Xiao-Guang. Opt. Quantum Electron. **55**, 97 (2023). https://doi.org/10.1007/s11082-022-04362-8
44. Fokas, A.S., Lenells, J.: The unified method: I. Nonlinearizable problems on the half-line. J. Phys. A. Math. Theor. (2012). https://doi.org/10.1088/1751-8113/45/19/195201
45. Islam, Z., Sheikh, M.A.N., Roshid, H.O., Hossain, M.A., Taher, M.A., Abdeljabbar, A.: Stability and Spin Solitonic Dynamics of the HFSC Model: Effects of Neighboring Interactions and

Crystal Field Anisotropy Parameters. Opt. Quantum Electron. **56**, 1–20 (2024). https://doi.org/10.1007/s11082-023-05739-z
46. Liang, X.F., Yang, J.M., Li, J., Xiao, L.F., Li, X.: Numerical simulation of irregular wave-simulating irregular wave train. J. Hydrodyn. **22**, 537–545 (2010). https://doi.org/10.1016/S1001-6058(09)60086-X
47. Hossain, M.N., Miah, M.M., Alosaimi, M., Alsharif, F., Kanan, M.: Exploring novel soliton solutions to the time-fractional coupled Drinfel ' d – Sokolov – Wilson equation in industrial engineering using two efficient techniques. Fractal and Fractional **8**, 352 (2024). https://doi.org/10.3390/fractalfract8060352
48. Rahman, R.U., Hammouch, Z., Alsubaie, A.S.A., Mahmoud, K.H., Alshehri, A., Az-Zo'bi, E.A., Osman, M.S.: Dynamical behavior of fractional nonlinear dispersive equation in Murnaghan's rod materials. Results in Physics **56**, 107207 (2024). https://doi.org/10.1016/j.rinp.2023.107207
49. Mase, H., Kirby, J.T.: Hybrid frequency-domain KdV equation for random wave transformation. Coast. Eng. **1993**, 474–487 (1992). https://doi.org/10.1142/9789814355524_0034
50. Hossain, M.N., Miah, M.M., Duraihem, F.Z., Rehman, S., Ma, W.-X.: Chaotic behavior, bifurcations, sensitivity analysis, and novel optical soliton solutions to the Hamiltonian amplitude equation in optical physics. Phys. Scr. **99**, 075231 (2024). https://doi.org/10.1088/1402-4896/ad52fd
51. Rafiq, M.H., Raza, N., Jhangeer, A.: Dynamic study of bifurcation, chaotic behavior and multi-soliton profiles for the system of shallow water wave equations with their stability. Chaos, Solitons & Fractals **171**, 113436 (2023). https://doi.org/10.1016/j.chaos.2023.113436
52. Rahman, M., Sun, M., Boulaaras, S., Baleanu, D.: Bifurcations, Chaotic behavior, sensitivity analysis, and various soliton solutions for the extended nonlinear Schrödinger equation. Bound. Value Probl. **2024**, (2024). https://doi.org/10.1186/s13661-024-01825-7

Authors and Affiliations

Md Nur Hossain[1,2] · I. Abouelfarag[3] · Abdulkafi Mohammed Saeed[4] · K. El-Rashidy[5] · M. Mamun Miah[6,7] · Wen-Xiu Ma[8,9,10]

✉ Md Nur Hossain
nur@ru.ac.bd

✉ M. Mamun Miah
mamun0954@gmail.com

✉ Wen-Xiu Ma
wma3@usf.edu

1 Department of Mathematics, University of Rajshahi, Rajshahi 6205, Bangladesh

2 Graduate School of Engineering, Osaka University, Suita, Osaka 565-0871, Japan

3 Mathematics Department, Khurmah University College, Taif University, Taif 21944, Saudi Arabia

4 Department of Mathematics, College of Science, Qassim University, Buraydah 51452, Saudi Arabia

5 Department of Mathematics, Faculty of Science, Beni-Suef University, Beni Suef 2722165, Egypt

6 Department of Applied Mathematics, University of Rajshahi, Rajshahi 6205, Bangladesh

7 Division of Mathematical and Physical Sciences, Kanazawa University, Kanazawa 9201192, Japan

8 Department of Mathematics, Zhejiang Normal University, Jinhua 321004, Zhejiang, China

9 Department of Mathematics and Statistics, University of South Florida, Tampa, FL 33620-5700, USA

10 Material Science Innovation and Modelling, North-West University, Mafikeng Campus, Private Bag, X2046, Mmabatho 2735, South Africa